Assessment of the Toxicity and Carcinogenicity of Double-Walled Carbon Nanotubes in the Rat Lung After Intratracheal Instillation: A Two-Year Study

Dina Mourad Saleh
Nagoya City University: Nagoya Shiritsu Daigaku https://orcid.org/0000-0002-8848-6708
Shengyong Luo
Anhui Medical University
Omnia Hosny Mohamed Ahmed
Nagoya City University: Nagoya Shiritsu Daigaku
David Bedell Alexander (dalexand@phar.nagoya-cu.ac.jp)
Nagoya City University: Nagoya Shiritsu Daigaku https://orcid.org/0000-0002-9017-3639
William T. Alexander
Nagoya City University: Nagoya Shiritsu Daigaku
Sivagami Gunasekaran
Nagoya City University: Nagoya Shiritsu Daigaku
Ahmed M. El-Gazzar
Alexandria University Faculty of Veterinary Medicine
Mohamed Abdelgied
Beni Suef University Faculty of Veterinary Medicine
Takamasa Numano
Nagoya City University: Nagoya Shiritsu Daigaku
Hiroshi Takase
Nagoya City University Graduate School of Medical Sciences and Medical School: Nagoya Shiritsu Daigaku Daigakuin Igaku Kenkyuka Igakubu
Makoto Ohnishi
Japan Bioassay Research Center
Susumu Tomono
Aichi Medical University School of Medicine
Randa Hussein Abd el Hadi
Assuit University, Faculty of Medicine
Katsumi Fukamachi
Nagoya City University Graduate School of Medical Sciences and Medical School: Nagoya Shiritsu Daigaku Daigakuin Igaku Kenkyuka Igakubu
Jun Kanno
National Institute of Hygienic Sciences
Akihiko Hirose
National Institute of Hygienic Sciences
Jiegou Xu

Anhui Medical University
Shugo Suzuki
Osaka City University Graduate School of Medicine
Aya Naiki
Nagoya City University Graduate School of Medical Sciences
Satoru Takahashi
Nagoya City University Graduate School of Medical Sciences
Hiroyuki Tsuda (htsuda@phar.nagoya-cu.ac.jp)
Nagoya City University: Nagoya Shiritsu Daigaku

Research Article

Keywords: Double Walled Carbon Nanotubes, two-year study, toxicity, carcinogenicity, rats

Posted Date: December 13th, 2021

DOI: https://doi.org/10.21203/rs.3.rs-1137913/v1

Version of Record: A version of this preprint was published at Particle and Fibre Toxicology on April 22nd, 2022. See the published version at https://doi.org/10.1186/s12989-022-00469-8.

Abstract

Background

Considering the expanding industrial applications of carbon nanotubes (CNTs), safety assessment of these materials is far less than needed. Very few long-term *in vivo* studies have been carried out. This is the first 2-year *in vivo* study to assess the effects of double walled carbon nanotubes (DWCNTs) in the lung and pleura of rats after pulmonary exposure.

Methods

Rats were divided into six groups: Untreated, Vehicle, 3 DWCNT groups (0.12mg/rat, 0.25mg/rat and 0.5mg/rat), and MWCNT-7 (0.5mg/rat). The test materials were administrated by intratracheal - intrapulmonary spraying (TIPS) every other day for 15 days. Rats were observed without further treatment until sacrifice at weeks 52 and 104.

Results

DWCNT were biopersistent in the rat lung and induced marked pulmonary inflammation with a significant increase in macrophage count and levels of the chemotactic cytokines CCL2 and CCL3. In addition, the 0.5 mg DWCNT treated rats had significantly higher pulmonary collagen deposition compared to the vehicle controls. The development of carcinomas in the lungs of rats treated with 0.5 mg DWCNT (4/24) was not quite statistically higher ($p = 0.0502$) than the vehicle control group (0/25), however, the overall incidence of lung tumor development, bronchiolo-alveolar adenoma and bronchiolo-alveolar carcinoma combined, in the lungs of rats treated with 0.5 mg DWCNT (7/24) was statistically higher ($p < 0.05$) than the vehicle control group (1/25). Notably, two of the rats treated with DWCNT, one in the 0.25 mg group and one in the 0.5mg group, developed pleural mesotheliomas. However, both of these lesions developed in the visceral pleura, and unlike the rats administered MWCNT-7, rats administered DWCNT did not have elevated levels of HMGB1 in their pleural lavage fluids.

Conclusions

Our results demonstrate that DWCNTs are biopersistent in the rat lung and induce chronic inflammation. Moreover, rats treated with 0.5 mg DWCNT developed pleural fibrosis. While our results do not show that DWCNT is carcinogenic in the rat lung, total tumor incidence was significantly increased in the 0.5 mg DWCNT group. Taken together, these findings demonstrate that the possibility that at least some types of DWCNTs are fibrogenic and carcinogenic cannot be ignored.

Background

Carbon nanotubes (CNTs) are composed of concentric one-atom thick graphene cylinders and have a wide range of applications [1]. The ability to manipulate the lengths and the number of graphene cylinders that compose CNTs has allowed the production of specific CNTs with different lengths and thicknesses, and these differences result in different CNTs having different physical properties. In general, CNTs are divided into two types single-walled carbon nanotubes (SWCNT) and multi-walled carbon nanotubes (MWCNTs) with double-walled carbon nanotubes (DWCNT)

sometimes being considered a distinct class of MWCNT. Multi-walled carbon nanotubes can be divided into two general subtypes, tangled and straight.

The very light weight of CNTs make them easily airborne and inhaled. Consequently, the possibility that CNTS may exhibit foreign body toxicity in the airways and pleura is of concern [2, 3, 4, 5, 6, 7]. Harmful fibrous particles like asbestos are known to induce fibrosis and cancer through chronic unresolved inflammation characterized by inflammatory cell accumulation and production of reactive oxygen and nitrogen spices (ROS & RNS) that can damage DNA and through repeated cycles of tissue damage and repair fix potentially transforming mutations into daughter cells [8, 9, 10, 11, 12, 13, 14].

Despite the widespread production and use of CNTs very few *in vivo* studies with a duration of 18 months or more have been carried out to assess the toxicity and carcinogenicity of these materials in experimental animals [15, 16, 17, 18, 19, 20, 21, 22]. At the time of this writing, IARC has evaluated only MWCNT-7 as carcinogenic in experimental animals and as being possibly carcinogenic in humans (Group 2B). All other CNTs had inadequate evidence in experimental animals for carcinogenicity and they were not classifiable as to their carcinogenicity to humans [10].

We have established an intratracheal intrapulmonary spraying (TIPS) method which we use to perform pulmonary toxicity studies [23]. Using TIPS, we assessed the toxicity and carcinogenicity of MWCNT-N, MWCNT-7, MWCNT-A, and MWCNT-B in long term studies. The thick straight MWCNT-N (40 layers) induced both lung tumors and malignant pleural mesotheliomas [19]; MWCNT-7 (more than 40 layers) induced malignant pleural mesotheliomas [21]; a thin tangled MWCNT, referred to as MWCNT-B, (15 layers) induced lung tumors [22]; and MWCNT-A (very thick 150 layers) was shown to be a likely lung carcinogen [22].

However, very little is known about the *in vivo* toxic effect of DWCNTs. The only available results are short term studies in mice and our short term study in rats. Crouzier et al. found inflammatory reactions 6, 24, and 48 hours after a single intranasal instillation of 1.5 mg/kg DWCNT (1.2 – 3.5 nm diameter, 1-10um length) [24]. Tian et al. found that inflammatory lesions were not resolved after a 7 day observation period after a single intratracheal instillation of 50 ug DWCNT (3.5 nm diameter, 1-10 um length) [25]. Sager et al. reported that mice administered 40 ug DWCNT (1-2 nm diameter, < 5 um length) by pharyngeal aspiration had developed alveolitis and lung fibrosis 56 days after administration of the DWCNT [26]. O'Shaughnessy et al. exposed mice to DWCNT by whole body inhalation at a dose of 10.8mg/m^3, 4h/day for 5 days. DWCNT caused inflammation and tissue injury to the lung [27]. El-Gazzer et al. administered DWCNT (1-3 nm diameter, due to the tangled nature of the fibers the length could not be measured) and MWCNT-7 (55.5±12 nm diameter, 6.5±2.4 um length) by TIPS. Six weeks after administration the degree of pulmonary and pleural toxicity induced by MWCNT-7 was much higher than that induced by DWCNT. DWCNT caused more extensive granulation tissue formation encapsulating the fibers than MWCNT-7 [28]. Based on these findings we conducted the present long-term study to assess the chronic toxicity and carcinogenicity of DWCNT in the rat lung.

Results

Characterization of the test substance

Representative SEM and TEM images of DWCNT and MWCNT fibers in suspension, prior to TIPS administration, are shown in Figure 1, and fiber lengths and diameters are presented in Table 1. DWCNT are thin and tangled and MWCNT are relatively thick and straight. Prior to TIPS administration, DWCNT fibers had a mean diameter of 14.32 ± 10.04 nm, and DWCNT recovered from lung tissue at 104 weeks had a mean diameter of 15.10 ± 13.99 nm. The

lengths of the DWCNT fibers could not be measured due to the tangled nature of the fibers. Prior to TIPS administration, MWCNT fibers had a diameter of 76.49 ± 31.14 nm and a mean length of 8.79 ± 4.41 um. MWCNT recovered from lung tissue at 104 weeks had a diameter of 69.42 ± 23.76 nm and a mean length of 8.45 ± 5.29 um. The size of the DWCNT and MWCNT-7 fibers recovered from the lung tissue at 104 weeks was not significantly different from the size of the fibers in suspension prior to TIPS administration.

Biodegradation of DWCNT and MWCNT-7 *in vitro*

DWCNT and MWCNT-7 were added to cultures of RAW cells, a mouse macrophage cell line, or to plates without cells. Plates were then incubated for 5 days. The effective lengths of the DWCNTs incubated without (control) and with RAW cells were estimated using far infrared absorption. The absorption peaks of both samples were observed around 20 cm^{-1} and the peak shift after incubation was within experimental error: this indicates that the changes in effective length between the controls and the DWCNTs incubated with RAW cells were below detectable limits and that the DWCNTs were not measurably damaged by incubation with RAW cells for 5 days (data not shown).

Macroscopic findings

The lungs of rats treated with 0.125, 0.25 and 0.5mg DWCNT showed grayish discoloration. The lungs of rats treated with 0.5 mg MWCNT-7 showed multiple dark black spots distributed throughout all lung lobes. The parabronchial and mediastinal lymph nodes of DWCNT groups were dark gray, and the lymph nodes of MWCNT-7 were entirely black.

Incidence of proliferative lesions and survival:

Table 2 shows the incidences of proliferative lesions at 52 weeks. No lung tumors were found in any of the rats sacrificed at 52 wk. One rat in the MWCNT-7 group developed a malignant pleural mesothelioma. The incidences of bronchioloalveolar hyperplasia (BAH) were significantly higher in the DWCNT 0.25 mg (5/6) ($p < 0.05$) and 0.5 mg (6/7) ($p < 0.05$) groups compared to the vehicle group (0/5). BAH in the DWCNT 0.25 and 0.5 mg groups was also significantly higher ($p < 0.05$) than in the MWCNT-7 group (1/7).

Table 3 shows the incidences of proliferative lesions at 104 weeks. There was an increase in both bronchioloalveolar adenomas (BAA) and bronchioloalveolar carcinomas (BAC) in the DWCNT groups compared with the vehicle control group. However, the development of carcinomas in the lungs of rats treated with 0.5 mg DWCNT (4/24) was not quite statistically higher ($p = 0.0502$) than the vehicle control group (0/25). On the other hand, the incidence of total lung tumors (BAA + BAC) in the DWCNT 0.5mg group (7/24) was significantly higher ($p < 0.05$) than the vehicle group (1/21). As expected, the incidence of malignant pleural mesothelioma in the MWCNT-7 group (16/25) was significantly higher ($p < 0.01$) than the vehicle group (0/21). One rat in the 0.25 mg DWCNT group and one rat in the 0.50 mg DWCNT group developed mesotheliomas, however, both of these mesotheliomas developed in the visceral pleura and as discussed below are unlikely to be relevant to human mesothelioma development. Two rats, one in the 0.125 mg DWCNT group and one in the 0.50 mg DWCNT group, also developed malignant peritoneal mesotheliomas, however, aged male Fischer 344 rats are prone to developing spontaneous peritoneal mesotheliomas [29]. Figure 2 shows typical lesions that developed in these rats. Other tumors including leukemia, pituitary tumors, mammary tumors, and scrotal malignant mesotheliomas were not treatment related.

No significant differences in the average survival time was observed between any of the DWCNT groups and the vehicle group. A significant decrease in survival time was observed in MWCNT-7 group compared to the other groups (Table 3, Additional File 1).

Histopathological evaluation

Table 4 shows pathological parameters at 52 weeks and Table 5 shows pathological parameters at 104 weeks.

Histopathological observation at 52 weeks and 104 weeks showed that DWCNTs were mostly phagocytosed by groups of macrophages forming foreign body granulation tissue (Figure 3), and at both time points granulation tissue was significantly increased in all treated group compared to the vehicle group. Granulation tissue was also significantly higher in the DWCNT 0.25 and 0.5 mg groups compared to MWCNT-7 group at week 52 and in the DWCNT 0.5 mg group compared to MWCNT-7 group at week 104. In contrast to DWCNT, MWCNT-7 fibers were commonly observed in free macrophages and some fibers were observed free in the alveolar space (Figure 3). Both DWCNT and MWCNT-7 fibers were found in the parabronchial and mediastinal lymph nodes (Figure 4).

Immunohistochemical evaluation showed that at 52 weeks and 104 weeks the CD68 positive macrophage count was significantly increased in all treated groups compared with the vehicle group (Tables 4 and 5). The macrophage count was also significantly increased in the DWCNT 0.25 and 0.5 mg groups compared to the MWCNT-7 group at both time points. Figure 5 shows CD68 immunostaining of vehicle, 0.5 mg DWCNT, and 0.5 MWCNT-7 lungs at 104 weeks.

Table 4 shows PCNA indices in the lung at 52 weeks. PCNA indices of alveolar cells in the rats administered DWCNT were not different from the controls at week 52. In contrast, PCNA indices of alveolar cells in the rats administered MWCNT were significantly increased compared to the controls at week 52.

Table 5 shows PCNA indices at 104 weeks, and Figure 5 shows PCNA immunostaining of vehicle, 0.5 mg DWCNT, and 0.5 MWCNT-7 lungs at 104 weeks. At 104 weeks, the PCNA index of alveolar cells was significantly increased in all treated groups compared with the vehicle group. The visceral and parietal pleural mesothelial PCNA indices were not increased in any of the DWCNT groups compared to the controls. The visceral and parietal pleural mesothelial PCNA indices were significantly higher in the MWCNT-7 group compared to the vehicle group and to the DWCNT groups.

Table 5 shows pulmonary and subpleural collagen deposition at 104 weeks, and Figure 5 shows Masson's trichrome staining of vehicle, 0.5 mg DWCNT, and 0.5 MWCNT-7 lungs at 104 weeks. At 104 weeks, fibrotic changes with increased deposition of collagen in the alveolar wall, parabronchial areas, within the granulation tissues, and in the visceral and parietal subpleural spaces were observed in the DWCNT and MWCNT-7 groups. Pulmonary collagen deposition was significantly higher in the DWCNT 0.5 mg and MWCNT-7 groups compared to the vehicle control group. Collagen deposition was somewhat increased in the visceral pleura but not in the parietal pleura of the 0.5 mg DWCNT group (Figure 6), and overall subpleural collagen deposition was not significantly increased in the 0.5 mg DWCNT group compared to the controls (Table 5). In contrast to the 0.5 mg DWCNT treated rats, MWCNT-7 treated rats had increased collagen deposition at the parietal pleura, and overall subpleural collagen deposition was significantly higher in the MWCNT-7 group than the vehicle controls and the 3 DWCNT groups.

The levels of CCL2 in lung tissue at 52 and 104 weeks are shown in Tables 4 and 5. The levels of CCL2 in lung tissues at 52 and 104 weeks were significantly higher in all treated groups compared with the vehicle control group. The CCL2 levels in the DWCNT 0.25 and 0.5 mg groups were significantly higher than the MWCNT-7 group at 52 weeks, and the CCL2 levels in the DWCNT 0.25 and 0.5 mg groups were significantly higher than the MWCNT-7 group at 104 weeks.

The levels of CCL3 in lung tissue at 52 and 104 weeks are shown in Tables 4 and 5. The levels of CCL3 in lung tissues at 52 and 104 weeks were significantly higher in all treated groups compared with the vehicle control group. The levels of CCL3 in the DWCNT 0.25 and 0.5 mg groups were significantly higher than the MWCNT-7 group at 52 weeks, and the levels of CCL3 in all three DWCNT groups were significantly higher than the MWCNT-7 group.

Lung fiber burden at 52 and 104 weeks

The lung fiber burden at 52 and 104 weeks is shown in Figure 7. At 52 weeks, the amounts of DWCNTs in the lungs were proportional to the initial dose administrated. Lung fiber burden decreased from week 52 to week 104, however, more than 1% of the initially instilled fibers remained in the lung 2 years after instillation and both DWCNT and MWCNT-7 were readily detectable in lung tissue sections (see Figures 3 and 5), indicating that DWCNT as well as MWCNT-7 was biopersistent in the rat lung.

Electron microscopic observation

TEM (Figure 8) and SEM (Figure 9) images at 104 weeks showed numerous thin DWCNTs engulfed by a single macrophage. DWCNT fibers were mostly engulfed by groups of macrophages forming granulation tissue with multinucleated giant cells (Figure 3). In contrast, TEM and SEM images primarily showed single MWCNT-7 fibers or small bundles of MWCNT-7 fibers associated with macrophages. MWCNT-7 fibers were also found free in the alveolar space (Figure 9). Importantly, MWCNT-7 fibers could also be seen penetrating the macrophage cell membrane (Figure 9).

DNA adductomes formation in the lung tissue

Additional file 2 shows adductome maps of rats at 52 weeks. The relative peak areas and the number of peaks are given for each group. There were no significant differences in either peak area or the number of peaks between any of the groups. No adducts specific to any of the treated groups were found.

HMBG1 levels in the pleural lavage fluid at week 104:

HMGB1 is a serum marker for mesothelioma [30, 31, 32, 33]. HMGB1 is released from mesothelial cells when they undergo necrosis induced by exposure to asbestos fibers [30, 34], and the released HMGB1 is involved in malignant transformation [32, 34, 35, 36, 37]. Therefore, the PLF of rats with malignant mesothelioma is expected to contain elevated levels of HMGB1. At 104 weeks, the PLF levels of HMGB1 were significantly elevated ($p < 0.001$) in the MWCNT-7 group (Figure 10). Notably, HMGB1 was not elevated the DWCNT treated groups, and as discussed below, these mesotheliomas developed in the visceral pleura and are unlikely to be relevant to human mesothelioma development.

Discussion

This is the first long-term, 2-year *in vivo* study to assess the toxicity and carcinogenicity of DWCNTs in the rat lung. Rats were untreated or administered vehicle or 0.125 mg, 0.25 mg, or 0.5 mg DWCNT per rat or 0.50 mg MWCNT-7 per rat: MWCNT-7 was used as the reference material. We found that DWCNTs were biopersistent in the rat lung and induced chronic inflammation, and that the 0.50 mg group developed lung fibrosis and lung tumors (see Tables 1 and 5). At 52 weeks, rats in the 0.25 mg and 0.50 mg groups had significantly elevated levels of hyperplasia in the lung, and at 104 weeks one rat in the 0.125 mg group and 2 rats in the 0.25 mg group and 4 rats in the 0.50 mg group had developed adenocarcinomas (see Tables 2 and 3). While these incidences were not statistically

significant compared to the vehicle controls, which did not develop adenocarcinomas, the apparent dose response agrees with the possibility that in this study DWCNTs may have had carcinogenic potential. In addition, the incidence of total lung tumors, bronchiolo-alveolar adenoma and bronchiolo-alveolar carcinoma combined, was significantly higher than the vehicle controls (see Table 3). Overall, these results indicate that the possibility that DWCNTs are carcinogenic cannot be ignored and that further long-term studies to assess the *in vivo* toxicity and carcinogenicity of DWCNT should be carried out.

It is notable that two rats administered DWCNT developed malignant pleural mesothelioma (see Table 3). The development of this tumor is rare in rats: the Japan Bioassay Research Center historical control data shows that approximately 1 of 1000 rats spontaneously develop malignant pleural mesothelioma and a retrospective review by Tokarz et al., 2021, identifies spontaneous primary pleural mesothelioma developing in approximately 1 of 2000 male F344 rats [38]. This suggests that development of these tumors is biologically significant. However, the PLF of the rats administered DWCNT did not have elevated levels of HMGB1. In contrast, the PLF of the rats administered MWCNT-7 did have elevated levels of HMGB1 (see Fig. 11). HMGB1 is released from mesothelial cells when they undergo necrosis induced by exposure to asbestos fibers [30, 34], and the released HMGB1 is involved in malignant transformation [32, 34, 35, 36, 37], suggesting that rats developing fiber-associated pleural mesothelioma would be expected to have elevated levels of HMGB1 in their PLF. In addition, HMGB1 is a serum marker for mesothelioma in humans [30, 31, 32, 33], suggesting that HMGB1 is also released from cells in patients with advanced mesothelioma. Therefore, the PLF of rats with either developing or advanced malignant pleural mesothelioma would be expected to contain elevated levels of HMGB1, as is the case for the rats administered MWCNT-7. The absence of elevated levels of HMGB1 in the groups administered DWCNT suggests that these lesions were not associated with fibers in the pleural cavity. Another notable point is that the pleural mesotheliomas that developed in the DWCNT administered rats developed in the visceral pleural. Fiber-associated pleural mesotheliomas are induced by fibers that are retained in the pleural cavity. These fibers are retained at the parietal pleura as they are carried by the pleural fluid that flows out of the pleural cavity through the stomata present in the parietal pleura, and consequently, fiber-associated pleural mesotheliomas initially develop in the parietal pleura [39, 40, 41, 42, 43, 44]. This also suggests that development of visceral mesothelioma in the DWNCT administered rats was not due to DWCNT fibers present in the pleural cavity. Finally, it is well known that the visceral pleura in rats is thin, consisting of the pleural mesothelial layer and a basement membrane lying directly over the alveoli (see Fig. 6 panel A), while in humans the visceral pleura has substantial submesothelial connective tissue. Consequently, in rats, but not in humans, interactions occurring in the lung alveoli adjacent to the visceral pleura could affect visceral pleural mesothelial cells, making the mechanism of visceral mesothelioma induction in rats not applicable to humans. Therefore, development of pleural mesothelioma in the visceral pleura coupled with the absence of elevated levels of HMGB1 in the PLF of the rats administered DWCNT support the premise that development of pleural mesothelioma in the DWCNT treated rats in the current study is not biologically relevant to humans.

Two rats also developed malignant peritoneal mesothelioma. However, aged male Fischer 344 rats are prone to developing spontaneous peritoneal mesotheliomas [29]. Therefore, the low incidence of these mesotheliomas suggests that they are not treatment related.

Another notable result in the present study is the low incidence of lung tumors in the MWCNT-7 treated rats: 2 rats developed lung carcinomas and 1 rat developed a lung adenoma. However, it needs to be noted that 16 rats in this group died before the end of the study due to mesotheliomas. Therefore, the incidence of lung tumor development in rats surviving to the end of the study (9 rats) was numerically higher than in the DWCNT groups. A low incidence of

lung tumor development has also been observed in a previous study in which rats administered MWCNT-7 by TIPS died before the end of the study period due to mesothelioma [21].

The DWCNT fibers used in the present study formed tangled agglomerates: agglomerate is used as defined by Walter 2013 [45]. Agglomerate formation is a known characteristic of CNTs [46, 47]. In the atmosphere of the working environment, CNTs are usually found as aggregates or agglomerates and rarely as single fibers [2, 48]. DWCNT agglomerates deposited beyond the ciliated airways were not completely moved out of the lung or broken down by alveolar macrophages (see Table 1 and Figure 7). It is well known that persistence of CNTs in the lung induces inflammation [2, 46, 47, 49, 50]. In our earlier study, at 6 weeks after administration of DWCNT to rats mild inflammation was observed and granulomas, which are an inflammatory sequestration response [51, 52], containing DWCNT fibers had developed [28]. In the present study, biopersistence of the DWCNT fibers in the rat lung induced persistent inflammation: at 52 and 104 weeks macrophage count, CCL2 and CCL3 expression, and granuloma formation was significantly elevated in the lungs of all DWCNT treated rats (Tables 4 and 5). Chronic inflammation is a hallmark of cancer [53, 54, 55, 56] and at 52 weeks hyperplasia was observed in the lungs of the 0.25 and 0.50 mg DWCNT treated rats and at 104 weeks the alveolar PCNA index was elevated in all DWCNT treated rats and tumor incidence was significantly increased the rats administered 0.5 mg DWCNT.

Fibrosis is characterized by the excess accumulation of the extracellular matrix (ECM) in response to non-resolving chronic inflammation [49, 50, 57, 58, 59]. Pulmonary fibrosis can impair lung function resulting in morbidity and mortality in humans [49, 57, 60]. During the chronic response to biopersistent CNTs, granulomas containing CNTs and characterized by local accumulation of activated macrophages serve as fibrogenic foci [57]. In our study, at 52 and 104 weeks all three groups of DWCNT treated rats had significant amounts of granulation tissue, increased macrophage counts, and elevated levels of CCL2 and CCL3, indicating the presence of activated macrophages, in the lung. Figure 5 shows collagen deposition at the fibrogenic foci formed by granulomas containing DWCNT and MWCNT-7 fibers. At 104 weeks elevated collagen deposition in the lung was observed in rats administered 0.25 and 0.50 mg DWCNT, and in the rats administered 0.50 mg DWCNT collagen deposition was significantly higher than the vehicle controls. In addition, fibrosis can be associated with tumorigenesis [50, 61], and in our study, the rats administered 0.50 mg DWCNT had significantly elevated collagen deposition and a significantly increased tumor incidence.

A final point regarding the results of the present study is how DWCNT can be tumorigenic in the rat lung but thin tangled CNTs do not induce the development of mesotheliomas, even when injected into the peritoneal cavity at relatively high levels [15, 16, 17]. One possible factor is the reported role of HMGB1 in the development of mesotheliomas [32, 34, 35, 36, 37]. Interaction of rigid fibers with mesothelial cells can result in cytotoxicity and release of HMGB1 from the cell, and the released HMGB1 can promote malignant transformation [32, 34, 35, 36, 37]. In contrast, thin tangled CNTs are reported to be less cytotoxic to mesothelial cells [62], and consequently, thin tangled fibers could be considerably less carcinogenic to mesothelium than rigid fibers.

As discussed above, the DWCNT fibers used in this study displayed characteristics typical of biopersistent fibers. As it is highly likely that individual DWCNT fibers would be phagocytosed and removed from the lung by alveolar macrophages, the biopersistence and subsequent induction of chromic inflammation, fibrosis, and tumorigenesis were the result of the agglomerates formed by the fibers. Since CNTs are typically found as aggregates of agglomerates and not as single fibers in the workplace [2], agglomerate formation by the DWCNT fibers used in the present study is not unexpected. Therefore, this characteristic must be taken into consideration when assessing the toxicity of CNTs, especially thin CNTs.

Conclusions

This is the first 2-year study to assess the toxicity and carcinogenicity of DWCNTs after administration into the rat lung. DWCNT did not induce toxic or carcinogenic effects in the pleural cavity, which is in agreement with long-term 2-year studies that found that rigid but not thin tangled CNTs induced mesothelioma when injected into the peritoneal cavity [15, 16, 17]. However, DWCNT administered at a dose of 0.5 mg/rat did cause pulmonary fibrosis and lung tumor development. This was most likely due to agglomerate formation by the fibers, resulting in biopersistence of the fibers in the lung and consequent chronic pulmonary inflammation which in turn promoted pulmonary fibrosis and tumor development. These results indicate that assessment of the toxicity of thin CNTs should not be based solely on the physiochemical characteristics of single fibers. In addition, the results of this study indicate that the possibility that DWCNTs may be toxic to humans cannot be ignored.

Methods

Nanomaterials

Two types of CNT were used in this study. DWCNT (brand name Tocana; Toray Industries ,Inc., Tokyo, Japan) with an iron content below detectable limits and water content equal to 0.025% by weight (information provided by the company) and MWCNT-7 (Mitsui Chemicals Inc., Tokyo, Japan) with an iron content of 0.3% by weight [63]**.** Table 6 shows the water and iron content of the fibers.

Animals

Nine-week old male F344 rats were purchased from Charles River Japan Inc. (Yukohama, Japan). The animals were housed in the Center for Experimental Animal Science of Nagoya City University Medical School, maintained on a 12 h light–dark cycle, and received Oriental MF basal diet (Oriental Yeast Co., Tokyo, Japan) and tap water *ad libitum*. The experimental protocol was approved by the Animal Care and Use Committee of Nagoya City University Medical School, and the research was conducted according to the Guidelines for the Care and Use of Laboratory Animals of Nagoya City University. The experiment was started after a 2-week acclimation and quarantine period.

Experimental design

A total of 180 rats 11 weeks old were divided into six groups of 30 animals each: Group 1, no treatment; Group 2, vehicle (saline with 0.5 % Pluronic F-68: Sigma-Aldrich Merck); Group 3, DWCNT (0.125 mg/rat); Group 4, DWCNT (0.25 mg/rat); Group 5, DWCNT (0.5 mg/rat); and Group 6, MWCNT-7 (0.5 mg/rat): MWCNT-7 was used as the reference material. Rats were administered the test solutions by TIPS as previously described [64]. Briefly, rats were anesthetized with 3% isoflurane and administered 0.5 ml vehicle or test material suspensions (15.6 ug , 31.25, or 62.5 µg of test material in 0.5 ml vehicle) using a micro sprayer (series IA–1B Intratracheal Aerosolizer Penn-century, Philadelphia, PA). Rats were administered one dose every other day over a 15-day period (8 administrations for total doses of 0.125, 0.25, or 0.5 mg DWCNT per rat and 0.5 mg MWCNT per rat). The amount of DWCNT administered to the rats was approximately equivalent to or less than the doses used in the studies by Crouzier et al., Tian et al., Sager et al., and El-Gazzar et al [24, 25, 26, 28]. The dose of MWCNT-7 was one third the amount of MWCNT-7 that caused mesothelioma in rats [21]. At week 52 an interim sacrifice was performed on 5 rats from the Untreated and Vehicle groups, 5 rats from the DWCNT 0.125mg/rat group, 7 rats from the DWCNT 0.25mg/rat group, 6 rats from the DWCNT-0.5 mg/rat group, and 5 rats from the MWCNT-7 group. After 52 weeks, animals that were found moribund were sacrificed, and the final sacrifice was at week 104.

Preparation of the test materials

Test materials were weighed and dispersed in tert-butyl alcohol by sonication for 10 min and stored frozen at -20˚C. Shortly before administration, the T-butyl alcohol was removed using an Eyela Freeze Drying machine (FDU-2110; Tokyo Rikakikai Co., Ltd., Tokyo, Japan), and the DWCNT and MWCNT-7 were suspended in saline containing 0.5% Pluronic F-68 (PF68, Sigma-Aldrich Merck) at 31.25, 62.5, and 125 μg/ml. After suspension in Saline + PF68, test materials were sonicated for 2 min four times at 3000 rpm using a polytron PT 1600E bench top homogenizer (Kinematika AG, Lattau, Switzerland). Immediately prior to administration, the suspensions were sonicated for 30 min using a Tomy Ultrasonic disruptor, UD-211, equipped with a TP-040 micro tip (Tomy Seiko Co., Ltd., Tokyo, Japan) at a power setting of 4.

Characterization of the test materials before and after TIPS administration

After sonication and before administration to the rats' lungs, 20 μl of each test material suspension was placed on a micro grid membrane pasting copper mesh (EMS 200-Cu, Nisshin EM Co., Ltd., Tokyo, Japan) for measurement of DWCNT and MWCNT-7 prior to TIPS administration. For measurement of DWCNT and MWCNT-7 in the lungs of rats at 52 and 104 weeks after instillation about 1 gm of paraformaldehyde fixed lung tissue was digested as previously described [65]. Briefly, tissues were incubated in Clean 99-K200® (Clean chemical Co., Ltd., Ibraki, Japan) overnight or until complete dissolution of lung tissues. The digested solution was then centrifuged at 12,000 rpm for 30 min and the supernatant was discarded. The pellet was resuspended in distilled water and lightly sonicated. The pellet was collected by centrifugation and washed two more times. After a final centrifugation, the pellet was resuspended in 200 μl of distilled water and the specimens were collected on EMD MilliporeTM Polycarbonate Membrane Filters (Millipore, Tokyo, Japan). Fibers were viewed by SEM (Field Emission Scanning Electronic Microscope; Hitachi High Technologies, Tokyo, Japan) at 5–10 kV and TEM (Transmission electron microscope; EDAX, Tokyo, Japan) at 15K-50K. Photos were analyzed by NIH image analyzer software (NIH, Bethesda, Maryland, USA). At least 200-300 fibers of each type of CNT were measured.

In vitro biodegradation

DWCNT and MWCNT-7 fibers were added to cultures of RAW cells, a mouse macrophage cell line, and to plates without cells (control). Cultures were incubated overnight with the CNTs at 37˚C in a humidified incubator. The cells were washed twice with PBS to remove materials not associated with the cells. Control plates were not handled. The cultures were then incubated for an addition 4 days. After 5 days incubation with CNTs, culture media was removed from the RAW cell cultures, and the cells were washed twice with PBS to remove materials not associated with the cells. The cells were then harvested and the CNTs recovered from the cells. For the control plates, the CNTs were collected from the cell-free culture media. The collected CNTs were measured using far-infrared absorption to estimate the effective CNT length [66].

Electron microscopic viewing of fibers in lung tissues

For high magnification viewing, H&E stained slides were immersed in xylene to remove the cover glass, dried, and processed for SEM (Model S Field Emission SEM; Hitachi High Technologies, Tokyo, Japan). For ultrafine viewing, a small piece of paraformaldehyde fixed lung tissue was imbedded in epoxy resin and processed for TEM (EDAX, Tokyo, Japan).

Measurement of DWCNT and MWCNTs in the lung

Measurement of the amount of CNT fibers in the lung tissue was performed as described previously [19, 65].

Tissue sample collection and histopathological examination

At necropsy, blood samples were collected via the abdominal aorta under deep isoflurane anesthesia and serum samples were stored at -80 °C. Organs, including lung, liver, kidney, spleen, brain, heart, and testes were examined for any macroscopic lesions. The trachea, esophagus, lymph nodes (including mediastinal lymph nodes), diaphragm including the diaphragmatic region of the parietal pleura were examined macroscopically and then processed and examined histopathologically.

The 4 right lobes of the lung of each rat were excised at necropsy, frozen in liquid nitrogen, and sored at – 80 degrees for further biochemical analysis. The remaining left lung was inflated and fixed with 4% paraformaldehyde solution in phosphate-buffered saline (PBS) adjusted to pH 7.3 and processed for light microscopic examination. H&E stained tissue sections were evaluated by two board-certified Pathologists of the Japanese society of Toxicologic pathology, Drs. Hiroyuki Tsuda and Satoru Takahashi, and diagnosis of hyperplasia, adenoma, adenocarcinoma, and mesothelioma was done according to the INHAND criteria [67].

PCNA staining of deparaffinized slides processed for antigen retrieval and blockade of endogenous peroxidase activity was performed as previously described [68]. For each lung specimen more than 1000 pulmonary epithelial cells and more than 500 visceral pleural and parietal pleural mesothelial cells were counted blindly in random fields. All nuclei showing brown staining of more than half of the nucleus were considered to be positive.

To determine the degree of inflammation the number of macrophages per cm^2 of lung tissue was determined: Deparaffinized slides processed for antigen retrieval and blockade of endogenous peroxidase activity were incubated with PBS containing 5% BSA and 5% goat serum for 1 h, then incubated with the macrophage marker anti-CD68 (BMA Biomedicals, August, Switzerland) diluted 1:2000 in PBS containing 1% BSA and 1% goat serum over- night at 4 °C. After overnight incubation, the slides were incubated with secondary antibody (Nichirei Biosciences, Tokyo, Japan) for 1 h, visualized with DAB (Nichirei Bio- sciences, Tokyo, Japan), and counterstained with hematoxylin. Light microscopic images representing at least one cm^2 from each lung were used to determine the density of the macrophages in the lungs.

Collagen deposition in lung tissues and visceral and partial pleura was quantified in light microscopic images of lung tissues and pleural sections stained with Masson's Trichrome (Abcam, Tokyo, Japan) using NIH image analyzer software (NIH, Besthesda, Meryland, USA): ten individual images were captured from 2 lung and 3 diaphragm sections from 3 rats per study group. Thresholding using pre-defined RGB criteria for collagen deposition was performed. This allowed collagen to be differentiated from alveolar tissue or pleural tissue. The surface area of fibrosed tissue was measured. Total lung alveolar and pleural tissue surface areas were measured individually by thresholding using predefined RGB criteria for lung alveolar and pleural tissues.The results are expressed as the percentage area of pulmonary collagen deposition per tissue surface area.

HMGB1 ELISA

At the final necropsy pleural lavage fluid collection was done for all rats as previously described [68]. High mobility group box protein 1 (HMGB1) was measured using a rat HMGB1 ELISA kit (Arigo Biolaboratories; ARG81310) according to the manufacturer's instructions.

CCL2 and CCL3 ELISA

Frozen right lung tissue samples (approximately 100 mg) were thawed and rinsed 3 times with ice-cold PBS and homogenized in 1 mL tissue protein extraction reagent (Thermo Scientific, Rockford, IL, USA) containing 1% (v/v) protease inhibitor cocktail (Sigma-Aldrich Merck). The homogenates were centrifuged at12000 g for 5 minutes at 4°C. Protein content of the supernatant was measured using the BCA Protein Assay Kit (Pierce Biotech). The levels of CCL2 and CCL3 in the supernatant were measured using a Rat MCP-1/CCL2 ELISA Kit (Sigma-Aldrich Merck; RAB0058) and a CCL3 ELISA Kit (LSBio; LS-F5526) according to the manufacturers' instructions.

Detection of DNA adductomes in the lung tissue

Rat lung DNA was extracted by Gentra® Puregene cell and tissue kit (Qiagen). The DNA (50 ug) was digested by incubation at 37°C for 12 h in 300 ul of 5 mM Tris-HCl (pH7.4) containing 50 units of DNase, 1 unit of Nuclease P1, 2 units of alkaline phosphatase, and 0.225 units of phosphodiesterase. After digestion, internal standards (100 pmol of 2',3'-dideoxyinosine and 2',3'-dideoxyadenosine) were added to the DNA hydrolysates. The hydrolysates were filtered through Amicon Ultra 3kDa centrifugal filters (Sigma-Aldrich Merck; Z677094), and 500 ul of methanol was added to the purified samples. After centrifugation and removal of the methanol, residual methanol was removed by evaporated *in vacuo*. DNA residues were dissolved in 100 ul of 50% methanol, and 10 ul of sample was subjected to LC/MS.

UHPLC-TOF-MS analyses was performed with a Shimadzu UHPLC Nexera X2 system (Shimadzu) using a Synergi Hydro-RP column (2.5 μm, 100 mm × 2 mm, Phenomenex) and Triple TOF 5600+ (SCIEX) with an electrospray ionization device running in the positive ion mode. The detector conditions were as follows: ion spray voltage at 5500 V, source temperature of 350°C, ion source gas 1, 60 psi, ion source gas 2 60 psi, declustering potential 80 V, collision energies of 45 V, and collision energy spread 15 V. Nitrogen was used as the collision gas. DNA adducts were detected using the MRM^{HR} mode. This strategy was designed to detect the neutral loss of 2'-deoxyribose from positively ionized 2'-deoxynucleoside adducts by monitoring the samples with $[M+H]^+ \rightarrow [M+H-116]^+$ transitions [69]. In the mobile phases used for LC-TOF-MS analyses, solvent A consisted of a 0.1% (v/v) solution of formic acid in water and solvent B consisted of a 0.1% (v/v) solution of formic acid in acetonitrile. The DNA adducts were eluted from the column using a linear gradient, which started at 95% solvent A and 5% solvent B, and progressed to 100% solvent B over a period of 10 min. The system was then eluted with 100% solvent B for 10 min before being returned to the initial conditions over a period of 10 min to allow for the equilibration of the column. The system was operated at a constant flow rate of 0.2 ml/min for all of the analyses.

Statistical analysis

Survival rates were analyzed using the Kaplan-Meier method. The incidences of bronchioloalveolar hyperplasia, bronchioloalveolar adenoma, bronchioloalveolar carcinoma, and total lung tumor incidences were analyzed for difference from vehicle controls using GraphPad's Fisher's extract test, and continuous data was analyzed using GraphPad's QuickCals t Test Calculator. All data are expressed as mean $\pm$ standard deviation. p-values < 0.05 were considered to be significant.

Declarations

Ethics approval and consent to participate

Not applicable

Consent for publication

Not applicable

Availability of data and materials

All data generated or analysed during this study are included in this published article and its supplementary information files.

Competing interests

The authors declare that they have no competing interests.

Funding

This study was supported by Research Grants from the Long-range Research Initiative (2017-2019) of the Japan Chemical Industry Association; Health and Labour Sciences Research Grants from the Ministry of Health, Labour and Welfare, Japan (H27-kagaku-shitei-004, H30-kagaku-shitei-004, H25-kagaku-ippan-004, H28-kagaku-ippan-004); YOG Specified Nonprofit Corporation, Association for Promotion of Research on Risk Assessment (2018-2021); and the Cultural Affairs and Missions Sector, Ministry of higher education of the Arab republic of Egypt.

Authors' contributions

DMS and WA helped prepare and administer the materials used in the study, directed pathological examination, collected and prepared tissue samples, analyzed tissue samples, and drafted and wrote the manuscript. SL, JX, SS, and AN contributed to the conception and design of the study and assisted in pathological examination. OHMA, SG, H Takase, and MO characterized the materials used in this study and characterized lung inflammation. DA helped prepare and administer the materials used in the study and assisted in writing the manuscript. AE-G and MA helped prepare and administer the materials used in the study and assisted in animal care and well-being. TN directed administration of the materials used in the study, collected and prepared tissue samples, and was in charge of animal care and well-being. S Tomono and KF contributed to the conception and design of the study and analyzed DNA adducts. RHAH contributed to the conception and design of the study and assisted in writing the manuscript. JK, AH, MO, and S Takahashi contributed to the conception and design of the study, assisted in pathological analysis and analysis of tissue samples, and assisted in writing the manuscript. H Tsuda acquired funding for the study, and contributed to the conception and design of the study, assisted in writing the manuscript, and gave final approval of the manuscript submitted for publication. All authors read and approved the final manuscript.

Acknowledgements

The authors would like to acknowledge Toray Industries Inc. Tokyo Japan for provision of DWCNT and Drs. Takahiro Morimoto and Toshiya Okazaki, CNT-Application Research Center, National Institute of Advanced Industrial Science and Technology (AIST) for measurement of DWCNT and MWCNT-7.

References

1. Ibrahim K. Carbon nanotubes-properties and applications: a review. Carbon letters. 2013;14:131-44. https://doi.org/10.5714/CL.2013.14.3.131.
2. Bergamaschi E, Garzaro G, Wilson Jones G, Buglisi M, Caniglia M, Godono A, et al. Occupational Exposure to Carbon Nanotubes and Carbon Nanofibres: More Than a Cobweb. Nanomaterials (Basel). 2021;11 3; doi:

10.3390/nano11030745. https://www.ncbi.nlm.nih.gov/pubmed/33809629.

3. Fadeel B, Kostarelos K. Grouping all carbon nanotubes into a single substance category is scientifically unjustified. Nat Nanotechnol. 2020;15 3:164; doi: 10.1038/s41565-020-0654-0. https://www.ncbi.nlm.nih.gov/pubmed/32123379.
4. Fischman M, Murashov V, Borak J, Seward J, Nanotechnology ATFo, Health. Nanotechnology and Health. J Occup Environ Med. 2019;61 3:e95-e8; doi: 10.1097/JOM.0000000000001548. https://www.ncbi.nlm.nih.gov/pubmed/30672766.
5. Hansen SF, Lennquist A. Carbon nanotubes added to the SIN List as a nanomaterial of Very High Concern. Nat Nanotechnol. 2020;15 1:3-4; doi: 10.1038/s41565-019-0613-9. https://www.ncbi.nlm.nih.gov/pubmed/31925393.
6. Heller DA, Jena PV, Pasquali M, Kostarelos K, Delogu LG, Meidl RE, et al. Banning carbon nanotubes would be scientifically unjustified and damaging to innovation. Nat Nanotechnol. 2020;15 3:164-6; doi: 10.1038/s41565-020-0656-y. https://www.ncbi.nlm.nih.gov/pubmed/32157238.
7. Schulte PA, Leso V, Niang M, Iavicoli I. Current state of knowledge on the health effects of engineered nanomaterials in workers: a systematic review of human studies and epidemiological investigations. Scand J Work Environ Health. 2019;45 3:217-38; doi: 10.5271/sjweh.3800. https://www.ncbi.nlm.nih.gov/pubmed/30653633.
8. Pollard KM. Silica, silicosis, and autoimmunity. Frontiers in immunology. 2016;7:97. https://doi.org/10.3389/fimmu.2016.00097
9. IARC. Arsenic, metals, fibres, and dusts. Volune 100C. 2012. http://monographs.iarc.fr/ENG/Monographs/vol100C/mono100C.pdf Accessed 02 Dec 2021.
10. IARC. Some nanomaterials and some fibres. Volume 111. 2017. http://monographs.iarc.fr/ENG/Monographs/vol111/mono111.pdf Accessed 02 Dec 2021.
11. Coussens LM, Werb Z. Inflammation and cancer. Nature. 2002;420 6917:860-7; doi: 10.1038/nature01322. https://www.ncbi.nlm.nih.gov/pubmed/12490959.
12. Okada F, Fujii J. Molecular mechanisms of inflammation-induced carcinogenesis. Journal of Clinical Biochemistry and Nutrition. 2006;39 3:103-13. https://doi.org/10.3164/jcbn.39.103
13. Topinka J, Loli P, Georgiadis P, Dusinska M, Hurbankova M, Kovacikova Z, et al. Mutagenesis by asbestos in the lung of lambda-lacI transgenic rats. Mutat Res. 2004;553 1-2:67-78; doi: 10.1016/j.mrfmmm.2004.06.023. https://www.ncbi.nlm.nih.gov/pubmed/15288534.
14. Yang H, Testa JR, Carbone M. Mesothelioma epidemiology, carcinogenesis, and pathogenesis. Curr Treat Options Oncol. 2008;9 2-3:147-57; doi: 10.1007/s11864-008-0067-z. https://www.ncbi.nlm.nih.gov/pubmed/18709470.
15. Muller J, Delos M, Panin N, Rabolli V, Huaux F, Lison D. Absence of carcinogenic response to multiwall carbon nanotubes in a 2-year bioassay in the peritoneal cavity of the rat. Toxicol Sci. 2009;110 2:442-8; doi: 10.1093/toxsci/kfp100. https://www.ncbi.nlm.nih.gov/pubmed/19429663.
16. Nagai H, Okazaki Y, Chew SH, Misawa N, Miyata Y, Shinohara H, et al. Intraperitoneal administration of tangled multiwalled carbon nanotubes of 15 nm in diameter does not induce mesothelial carcinogenesis in rats. Pathol Int. 2013;63 9:457-62; doi: 10.1111/pin.12093, https://doi.org/10.1111/pin.12093
17. Rittinghausen S, Hackbarth A, Creutzenberg O, Ernst H, Heinrich U, Leonhardt A, et al. The carcinogenic effect of various multi-walled carbon nanotubes (MWCNTs) after intraperitoneal injection in rats. Part Fibre Toxicol. 2014;11:59; doi: 10.1186/s12989-014-0059-z.

18. Kasai T, Umeda Y, Ohnishi M, Mine T, Kondo H, Takeuchi T, et al. Lung carcinogenicity of inhaled multi-walled carbon nanotube in rats. Part Fibre Toxicol. 2016;13 1:53; doi: 10.1186/s12989-016-0164-2. https://www.ncbi.nlm.nih.gov/pubmed/27737701.
19. Suzui M, Futakuchi M, Fukamachi K, Numano T, Abdelgied M, Takahashi S, et al. Multiwalled carbon nanotubes intratracheally instilled into the rat lung induce development of pleural malignant mesothelioma and lung tumors. Cancer Sci. 2016;107 7:924-35; doi: 10.1111/cas.12954. https://www.ncbi.nlm.nih.gov/pubmed/27098557.
20. Honda K, Naya M, Takehara H, Kataura H, Fujita K, Ema M. A 104-week pulmonary toxicity assessment of long and short single-wall carbon nanotubes after a single intratracheal instillation in rats. Inhal Toxicol. 2017;29 11:471-82; doi: 10.1080/08958378.2017.1394930. https://www.ncbi.nlm.nih.gov/pubmed/29110549.
21. Numano T, Higuchi H, Alexander DB, Alexander WT, Abdelgied M, El-Gazzar AM, et al. MWCNT-7 administered to the lung by intratracheal instillation induces development of pleural mesothelioma in F344 rats. Cancer Sci. 2019;110 8:2485-92; doi: 10.1111/cas.14121. https://www.ncbi.nlm.nih.gov/pubmed/31265162.
22. Saleh DM, Alexander WT, Numano T, Ahmed OHM, Gunasekaran S, Alexander DB, et al. Comparative carcinogenicity study of a thick, straight-type and a thin, tangled-type multi-walled carbon nanotube administered by intra-tracheal instillation in the rat. Part Fibre Toxicol. 2020;17 1:48; doi: 10.1186/s12989-020-00382-y. https://www.ncbi.nlm.nih.gov/pubmed/33054855.
23. Tsuda H, Alexander DB. Development of Intratracheal Intrapulmonary Spraying (TIPS) Administration as a Feasible Assay Method for Testing the Toxicity and Carcinogenic Potential of Multiwall Carbon Nanotubes. In Vivo Inhalation Toxicity Screening Methods for Manufactured Nanomaterials: Springer; 2019. p. 145-63.
24. Crouzier D, Follot S, Gentilhomme E, Flahaut E, Arnaud R, Dabouis V, et al. Carbon nanotubes induce inflammation but decrease the production of reactive oxygen species in lung. Toxicology. 2010;272 1-3:39-45; doi: 10.1016/j.tox.2010.04.001. https://doi.org/10.1016/j.tox.2010.04.001
25. Tian F, Habel NC, Yin R, Hirn S, Banerjee A, Ercal N, et al. Pulmonary DWCNT exposure causes sustained local and low-level systemic inflammatory changes in mice. Eur J Pharm Biopharm. 2013;84 2:412-20; doi: 10.1016/j.ejpb.2013.03.008. https://doi.org/10.1016/j.ejpb.2013.03.008
26. Sager TM, Wolfarth MW, Battelli LA, Leonard SS, Andrew M, Steinbach T, et al. Investigation of the pulmonary bioactivity of double-walled carbon nanotubes. J Toxicol Environ Health A. 2013;76 15:922-36; doi: 10.1080/15287394.2013.825571. https://doi.org/10.1080/15287394.2013.825571
27. O'Shaughnessy PT, Adamcakova-Dodd A, Altmaier R, Thorne PS. Assessment of the Aerosol Generation and Toxicity of Carbon Nanotubes. Nanomaterials (Basel). 2014;4 2:439-53; doi: 10.3390/nano4020439. https://doi.org/10.3390/nano4020439
28. El-Gazzar AM, Abdelgied M, Alexander DB, Alexander WT, Numano T, Iigo M, et al. Comparative pulmonary toxicity of a DWCNT and MWCNT-7 in rats. Arch Toxicol. 2019;93 1:49-59; doi: 10.1007/s00204-018-2336-3. https://www.ncbi.nlm.nih.gov/pubmed/30341734.
29. Blackshear PE, Pandiri AR, Ton TV, Clayton NP, Shockley KR, Peddada SD, et al. Spontaneous mesotheliomas in F344/N rats are characterized by dysregulation of cellular growth and immune function pathways. Toxicol Pathol. 2014;42 5:863-76; doi: 10.1177/0192623313501894. https://www.ncbi.nlm.nih.gov/pubmed/23980201.
30. Napolitano A, Antoine DJ, Pellegrini L, Baumann F, Pagano I, Pastorino S, et al. HMGB1 and Its Hyperacetylated Isoform are Sensitive and Specific Serum Biomarkers to Detect Asbestos Exposure and to Identify Mesothelioma Patients. Clin Cancer Res. 2016;22 12:3087-96; doi: 10.1158/1078-0432.CCR-15-1130. https://www.ncbi.nlm.nih.gov/pubmed/26733616.

31. Tabata C, Shibata E, Tabata R, Kanemura S, Mikami K, Nogi Y, et al. Serum HMGB1 as a prognostic marker for malignant pleural mesothelioma. BMC Cancer. 2013;13:205; doi: 10.1186/1471-2407-13-205. https://www.ncbi.nlm.nih.gov/pubmed/23617783.
32. Wang Y, Jiang Z, Yan J, Ying S. HMGB1 as a Potential Biomarker and Therapeutic Target for Malignant Mesothelioma. Dis Markers. 2019;2019:4183157; doi: 10.1155/2019/4183157. https://www.ncbi.nlm.nih.gov/pubmed/30891101.
33. Ying S, Jiang Z, He X, Yu M, Chen R, Chen J, et al. Serum HMGB1 as a Potential Biomarker for Patients with Asbestos-Related Diseases. Dis Markers. 2017;2017:5756102; doi: 10.1155/2017/5756102. https://www.ncbi.nlm.nih.gov/pubmed/28348451.
34. Yang H, Rivera Z, Jube S, Nasu M, Bertino P, Goparaju C, et al. Programmed necrosis induced by asbestos in human mesothelial cells causes high-mobility group box 1 protein release and resultant inflammation. Proc Natl Acad Sci U S A. 2010;107 28:12611-6; doi: 10.1073/pnas.1006542107. https://www.ncbi.nlm.nih.gov/pubmed/20616036.
35. Jube S, Rivera ZS, Bianchi ME, Powers A, Wang E, Pagano I, et al. Cancer cell secretion of the DAMP protein HMGB1 supports progression in malignant mesothelioma. Cancer Res. 2012;72 13:3290-301; doi: 10.1158/0008-5472.CAN-11-3481. https://www.ncbi.nlm.nih.gov/pubmed/22552293.
36. Qi F, Okimoto G, Jube S, Napolitano A, Pass HI, Laczko R, et al. Continuous exposure to chrysotile asbestos can cause transformation of human mesothelial cells via HMGB1 and TNF-alpha signaling. Am J Pathol. 2013;183 5:1654-66; doi: 10.1016/j.ajpath.2013.07.029. https://www.ncbi.nlm.nih.gov/pubmed/24160326.
37. Xue J, Patergnani S, Giorgi C, Suarez J, Goto K, Bononi A, et al. Asbestos induces mesothelial cell transformation via HMGB1-driven autophagy. Proc Natl Acad Sci U S A. 2020;117 41:25543-52; doi: 10.1073/pnas.2007622117. https://www.ncbi.nlm.nih.gov/pubmed/32999071.
38. Tokarz DA, Gruebbel MM, Willson GA, Hardisty JF, Pearse G, Cesta MF. Spontaneous Primary Pleural Mesothelioma in Fischer 344 (F344) and Other Rat Strains: A Retrospective Review. Toxicol Pathol. 2021:1926233211053631; doi: 10.1177/01926233211053631. https://www.ncbi.nlm.nih.gov/pubmed/34727809.
39. Chew SH, Toyokuni S. Malignant mesothelioma as an oxidative stress-induced cancer: An update. Free Radic Biol Med. 2015;86:166-78; doi: 10.1016/j.freeradbiomed.2015.05.002. https://www.ncbi.nlm.nih.gov/pubmed/25975982.
40. Donaldson K, Murphy FA, Duffin R, Poland CA. Asbestos, carbon nanotubes and the pleural mesothelium: a review of the hypothesis regarding the role of long fibre retention in the parietal pleura, inflammation and mesothelioma. Part Fibre Toxicol. 2010;7:5; doi: 10.1186/1743-8977-7-5. https://www.ncbi.nlm.nih.gov/pubmed/20307263.
41. Donaldson K, Poland CA, Murphy FA, MacFarlane M, Chernova T, Schinwald A. Pulmonary toxicity of carbon nanotubes and asbestos - similarities and differences. Adv Drug Deliv Rev. 2013;65 15:2078-86; doi: 10.1016/j.addr.2013.07.014. https://www.ncbi.nlm.nih.gov/pubmed/23899865.
42. Miserocchi G, Sancini G, Mantegazza F, Chiappino G. Translocation pathways for inhaled asbestos fibers. Environ Health. 2008;7:4; doi: 10.1186/1476-069X-7-4. https://www.ncbi.nlm.nih.gov/pubmed/18218073.
43. Roe OD, Stella GM. Malignant pleural mesothelioma: history, controversy and future of a manmade epidemic. Eur Respir Rev. 2015;24 135:115-31; doi: 10.1183/09059180.00007014. https://www.ncbi.nlm.nih.gov/pubmed/25726562.

44. Stellaa GM. Carbon nanotubes and pleural damage: perspectives of nanosafety in the light of asbestos experience. Biointerphases. 2011; 6, P1-P17. https://doi.org/10.1116/1.3582324
45. Walter D. Primary particles–agglomerates–aggregates. Nanomaterials. 2013:9-24. https://onlinelibrary.wiley.com/doi/pdf/10.1002/9783527673919.oth1#page=9. Accessed 02 Dec 2021.
46. Johnston HJ, Hutchison GR, Christensen FM, Peters S, Hankin S, Aschberger K, et al. A critical review of the biological mechanisms underlying the in vivo and in vitro toxicity of carbon nanotubes: The contribution of physico-chemical characteristics. Nanotoxicology. 2010;4 2:207-46; doi: 10.3109/17435390903569639. https://www.ncbi.nlm.nih.gov/pubmed/20795897.
47. Laux P, Riebeling C, Booth AM, Brain JD, Brunner J, Cerrillo C, et al. Biokinetics of Nanomaterials: the Role of Biopersistence. NanoImpact. 2017;6:69-80; doi: 10.1016/j.impact.2017.03.003. https://www.ncbi.nlm.nih.gov/pubmed/29057373.
48. Dahm MM, Schubauer-Berigan MK, Evans DE, Birch ME, Fernback JE, Deddens JA. Carbon Nanotube and Nanofiber Exposure Assessments: An Analysis of 14 Site Visits. Ann Occup Hyg. 2015;59 6:705-23; doi: 10.1093/annhyg/mev020. https://www.ncbi.nlm.nih.gov/pubmed/25851309.
49. Dong J. Microenvironmental Alterations in Carbon Nanotube-Induced Lung Inflammation and Fibrosis. Front Cell Dev Biol. 2020;8:126; doi: 10.3389/fcell.2020.00126. https://www.ncbi.nlm.nih.gov/pubmed/32185174.
50. Dong J, Ma Q. Integration of inflammation, fibrosis, and cancer induced by carbon nanotubes. Nanotoxicology. 2019;13 9:1244-74; doi: 10.1080/17435390.2019.1651920. https://www.ncbi.nlm.nih.gov/pubmed/31537143.
51. Ito T, Connett JM, Kunkel SL, Matsukawa A. The linkage of innate and adaptive immune response during granulomatous development. Front Immunol. 2013;4:10; doi: 10.3389/fimmu.2013.00010. https://doi.org/10.3389/fimmu.2013.00010
52. Petersen HJ, Smith AM. The role of the innate immune system in granulomatous disorders. Front Immunol. 2013;4:120; doi: 10.3389/fimmu.2013.00120. https://doi.org/10.3389/fimmu.2013.00120
53. Barbarino M, Giordano A. Assessment of the Carcinogenicity of Carbon Nanotubes in the Respiratory System. Cancers (Basel). 2021;13 6; doi: 10.3390/cancers13061318. https://www.ncbi.nlm.nih.gov/pubmed/33804168.
54. Cavallo F, De Giovanni C, Nanni P, Forni G, Lollini PL. 2011: the immune hallmarks of cancer. Cancer Immunol Immunother. 2011;60 3:319-26; doi: 10.1007/s00262-010-0968-0. https://www.ncbi.nlm.nih.gov/pubmed/21267721.
55. Colotta F, Allavena P, Sica A, Garlanda C, Mantovani A. Cancer-related inflammation, the seventh hallmark of cancer: links to genetic instability. Carcinogenesis. 2009;30 7:1073-81; doi: 10.1093/carcin/bgp127. https://www.ncbi.nlm.nih.gov/pubmed/19468060.
56. Hanahan D, Weinberg RA. Hallmarks of cancer: the next generation. Cell. 2011;144 5:646-74; doi: 10.1016/j.cell.2011.02.013. https://www.ncbi.nlm.nih.gov/pubmed/21376230.
57. Dong J, Ma Q. Type 2 Immune Mechanisms in Carbon Nanotube-Induced Lung Fibrosis. Front Immunol. 2018;9:1120; doi: 10.3389/fimmu.2018.01120. https://www.ncbi.nlm.nih.gov/pubmed/29872441.
58. Dong J, Ma Q. In Vivo Activation and Pro-Fibrotic Function of NF-kappaB in Fibroblastic Cells During Pulmonary Inflammation and Fibrosis Induced by Carbon Nanotubes. Front Pharmacol. 2019;10:1140; doi: 10.3389/fphar.2019.01140. https://www.ncbi.nlm.nih.gov/pubmed/31632276.
59. Wynn TA. Cellular and molecular mechanisms of fibrosis. J Pathol. 2008;214 2:199-210; doi: 10.1002/path.2277. https://www.ncbi.nlm.nih.gov/pubmed/18161745.

60. Sayan M, Mossman BT. The NLRP3 inflammasome in pathogenic particle and fibre-associated lung inflammation and diseases. Part Fibre Toxicol. 2016;13 1:51; doi: 10.1186/s12989-016-0162-4.
61. Kane AB, Organization WH. Mechanisms of fibre carcinogenesis. 2000. IARC Scientific Publications No. 140.
62. Nagai H, Okazaki Y, Chew SH, Misawa N, Yamashita Y, Akatsuka S, et al. Diameter and rigidity of multiwalled carbon nanotubes are critical factors in mesothelial injury and carcinogenesis. Proc Natl Acad Sci U S A. 2011;108 49:E1330-8; doi: 10.1073/pnas.1110013108. https://doi.org/10.1073/pnas.1110013108
63. Sakamoto Y, Hojo M, Kosugi Y, Watanabe K, Hirose A, Inomata A, et al. Comparative study for carcinogenicity of 7 different multi-wall carbon nanotubes with different physicochemical characteristics by a single intraperitoneal injection in male Fischer 344 rats. J Toxicol Sci. 2018;43 10:587-600; doi: 10.2131/jts.43.587. https://doi.org/10.2131/jts.43.587
64. Abdelgied M, El-Gazzar AM, Alexander WT, Numano T, Iigou M, Naiki-Ito A, et al. Carcinogenic effect of potassium octatitanate (POT) fibers in the lung and pleura of male Fischer 344 rats after intrapulmonary administration. Particle and Fibre Toxicology. 2019;16 1:34; doi: 10.1186/s12989-019-0316-2. https://doi.org/10.1186/s12989-019-0316-2.
65. Ohnishi M, Yajima H, Kasai T, Umeda Y, Yamamoto M, Yamamoto S, et al. Novel method using hybrid markers: development of an approach for pulmonary measurement of multi-walled carbon nanotubes. J Occup Med Toxicol. 2013;8 1:30; doi: 10.1186/1745-6673-8-30. https://doi.org/10.1186/1745-6673-8-30
66. Morimoto T, Joung SK, Saito T, Futaba DN, Hata K, Okazaki T. Length-dependent plasmon resonance in single-walled carbon nanotubes. ACS Nano. 2014;8 10:9897-904; doi: 10.1021/nn505430s. https://www.ncbi.nlm.nih.gov/pubmed/25283493.
67. Renne R, Brix A, Harkema J, Herbert R, Kittel B, Lewis D, et al. Proliferative and nonproliferative lesions of the rat and mouse respiratory tract. Toxicol Pathol. 2009;37 7 Suppl:5s-73s; doi: 10.1177/0192623309353423. https://doi.org/10.1177/0192623309353423
68. Abdelgied M, El-Gazzar AM, Alexander DB, Alexander WT, Numano T, Iigou M, et al. Potassium octatitanate fibers induce persistent lung and pleural injury and are possibly carcinogenic in male Fischer 344 rats. Cancer science. 2018;109 7:2164-77. https://doi.org/10.1111/cas.13643
69. Kanaly RA, Matsui S, Hanaoka T, Matsuda T. Application of the adductome approach to assess intertissue DNA damage variations in human lung and esophagus. Mutat Res. 2007;625 1-2:83-93; doi: 10.1016/j.mrfmmm.2007.05.006. https://www.ncbi.nlm.nih.gov/pubmed/17606272.

Tables

Table 1: Size of DWCNT and MWCNT-7 aggregates in the vehicle before dosing and at week 104

	Length before dosing	Length at 104 weeks	Diameter before dosing	Diameter at 104 weeks
DWCNT	NA [a]	NA [a]	14.32 + 10.04 nm	15.10+ 13.99 nm
MWCNT-7	8.79 + 4.41 um	8.45 + 5.29 um	76.49 + 31.14 nm	69.42 + 23.76 nm

[a] Not available (unable to measure DWCNT fiber length because of agglomerate formation)

Table 2: Incidence of proliferative and neoplastic lesions at 52 weeks

	Untreated	Vehicle	DWCNT 0.125 mg/rat	DWCNT 0.250 mg/rat	DWCNT 0.500 mg/rat	MWCNT 0.500mg/rat
Number of rats examined	5	5	5	7	6	5
Bronchiolo- alveolar Hyperplasia (BAH)	0	0	2	5*,#	5*,#	1
Pleural Mesothelioma	0	0	0	0	0	1

*Difference from Vehicle group: $p < 0.05$

Difference from MWCNT-7 group: $p < 0.05$

No lung tumors were found in any of the rats sacrificed at 52 wk.

Table 3 : Incidence of proliferative lesions at 104 weeks

	Untreated	Vehicle	DWCNT 0.125 mg/rat	DWCNT 0.250 mg/rat	DWCNT 0.500 mg/rat	MWCNT 0.500mg/rat
Rats Examined	21	25	25	26	24	25
Mean survival ± S.D (weeks)	94.9 ± 3.5	89.7 ± 6.4	90.3 ± 4.6	94.3 ± 4.3	93.9 ± 5.0	74.9 ± 10.3$ #
Bronchiolo-alveolar hyperplasia (BAH)	4	4	1	4	0	1
Bronchiolo-alveolar adenoma (BAA)	1	1	3	2	3	1
Bronchiolo-alveolar adenocarcinoma (BAC)	0	0	1	2	4	2
BAA + BAC	1	1	4	4	7*	3
Malignant pleural mesothelioma	0	0	0	1[a]	1[a]	16***
Malignant peritoneal mesothelioma	0	0	1	0	1	0

$,# Significantly different from the vehicle group and DWCNT treated groups: $p < 0.05$

*,*** Significantly different from the vehicle group: $p < 0.05$ and 0.001

[a] The malignant pleural mesothelioma developed in the visceral pleura.

Table 4: Cell proliferation and inflammation related parameters in the lung tissue at 52 weeks

	Untreated	Vehicle	DWCNT 0.125 mg/rat	DWCNT 0.250 mg/rat	DWCNT 0.500 mg/rat	MWCNT 0.500mg/rat
Granulation Tissue count/cm^2 mean ± S.D	1.1 ± 0.35	2.4 ± 1.2	98.8 ± 31.0***	189 ± 32.5***,#	404.4 ± 88.8***,#	65.4 ± 11.8**
Macrophage count/cm^2 mean ± S.D	1.45± 0.23	6.93±1.47	21.72±4.2***	33.01±6.4***,#	49.1±5.79***,#	15.88±5.79**
Alveolar cell PCNA index %	10.70	18.00	16.50	17.80	25.80	44.52 **
CCL2 pg/mg lung protein mean ± S.D	3.30±0.28	3.65±0.44	16.69±4.65***	23.36±4.33***,#	22.37±3.7***,#	9.49±0.98***
CCL3 pg/mg lung protein mean ± S.D	6.82±0.56	8.19±0.73	40.32±10.4**	69.09±7.84***,#	135.57±11***,##	24.86±8.4*

*,**,*** Difference from the Vehicle group at $p < 0.05$, 0.01, 0.001, respectively.

#,## Significantly increased compared to MWCNT-7 at $p < 0.05$, 0.01 respectively.

Table 5: Cell proliferation and inflammation related parameters of the lung tissue at 104 weeks

	Untreated	Vehicle	DWCNT 0.125 mg/rat	DWCNT 0.250 mg/rat	DWCNT 0.500 mg/rat	MWCNT 0.500mg/rat
Granulation Tissue count/cm^2 mean ±S.D	0.9 ± 0.3	1.3 ± 0.6	50.9 ± 5.2**	118.9 ± 68.8***	365.1 ± 81.7***,#	94.9 ± 35.3**
Macrophage count/cm^2 mean ± S.D	54.6 ± 16.4	75 ± 23.0	361.8 ± 53.4***	502.8 ± 59.1***,#	479.1 ± 48.2***,#	314.7 ± 91.6***
Alveolar PCNA index %	3.60	4.48	8.82*	18.54 **	21.20**#	14.10**
Visceral pleural PCNA index %	0.20	0.36	0.44	1.40	1.32	15.20**$
Parietal pleural PCNA index %	2	2.3	2	1.9	2.6	23.75***$
Pulmonary Collagen deposition %[a]	13.04	8.50	13	18.15	20.47*	27*
Supleural Collagen deposition % [b]	4.20	2.25	5.50	4.45	16.87	64.20***$
CCL2 ng/mg lung protein mean ± S.D	0.77 ± 0.3	1.6 ± 0.87	6.67 ± 2.44***	8.40 ± 1.73***,#	10.74±1.94***,##	5.20 ± 1.6***
CCL3 ng/mg lung protein mean ± S.D	0.58 ± 0.27	0.55 ± 0.16	0.71 ± 0.16*,#	0.75 ± 0.21*,#	0.74 ± 0.19*,#	0.52 ± 0.12

*,**,*** Significantly increased from the Vehicle at p < 0.05, 0.01, 0.001 respectively.

#,## Significantly increased compared to MWCNT-7 at p <0.05, 0.01 respectively.

$ Significantly increased in compared to DWCNT groups: p <0.01.

[a] Results are expressed as the percentage area of pulmonary collagen deposition/total alveolar tissue area.

[b] Results are expressed as the percentage area of subpleural collagen deposition/total pleural tissue area.

Table 6: Iron and water content of DWCNT and MWCNT-7 before dosing

	Iron content（wt％）	Water content（wt％）
DWCNT	0[a]	0.025[a]
MWCNT-7	0.3[b]	NA [c]

[a] Information provided by Toray the manufacturer company .

[b] Sakamoto et al. 2018 [63]

[c] Not available

Figures

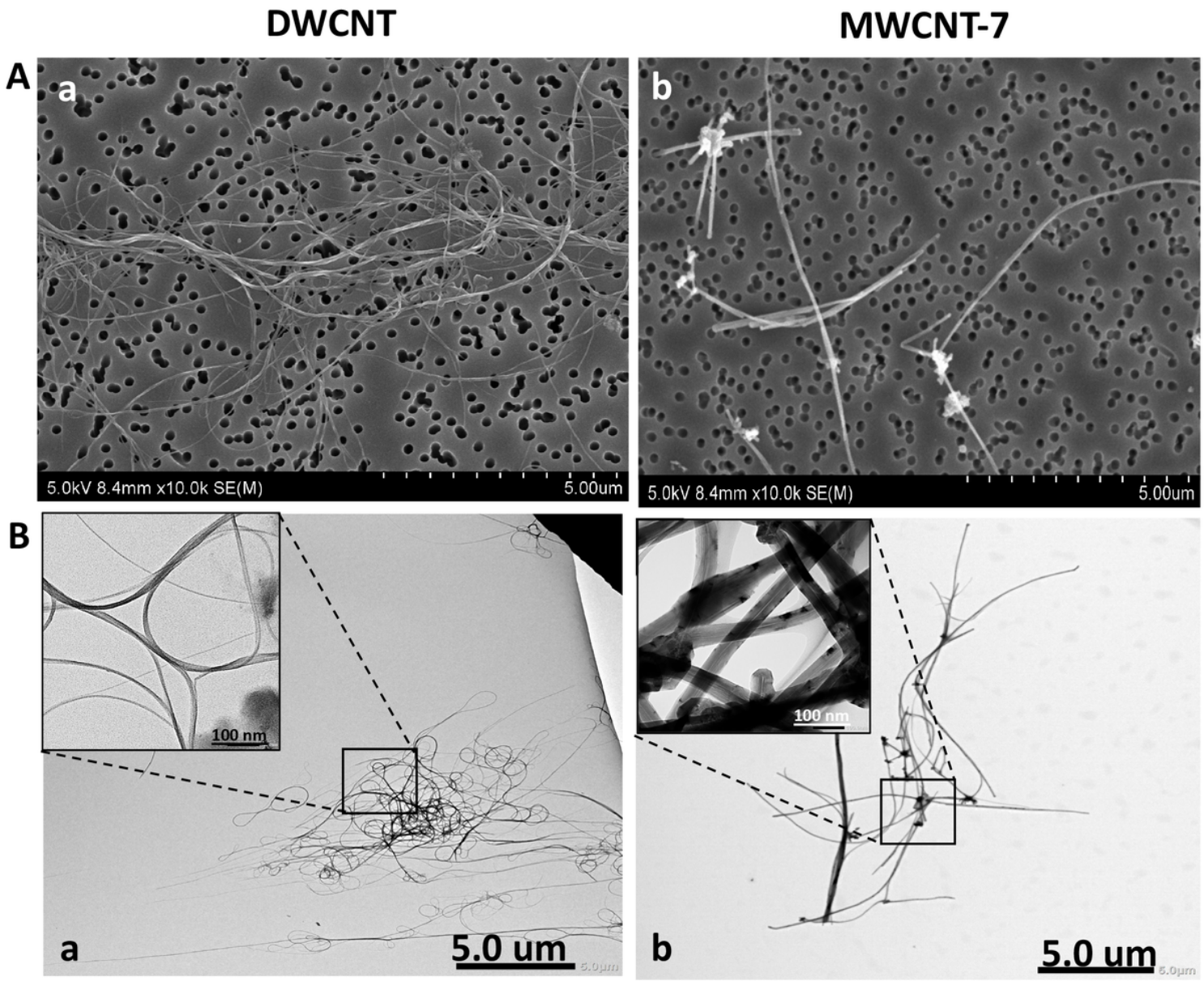

Figure 1

Characterization of test materials in suspension. Panel A shows scanning electron microscopy images of (a) DWCNT and (b) MWCNT-7 fibers and panel B shows transmission electron microscopy images of (a) DWCNT and (b) MWCNT-7 fibers.

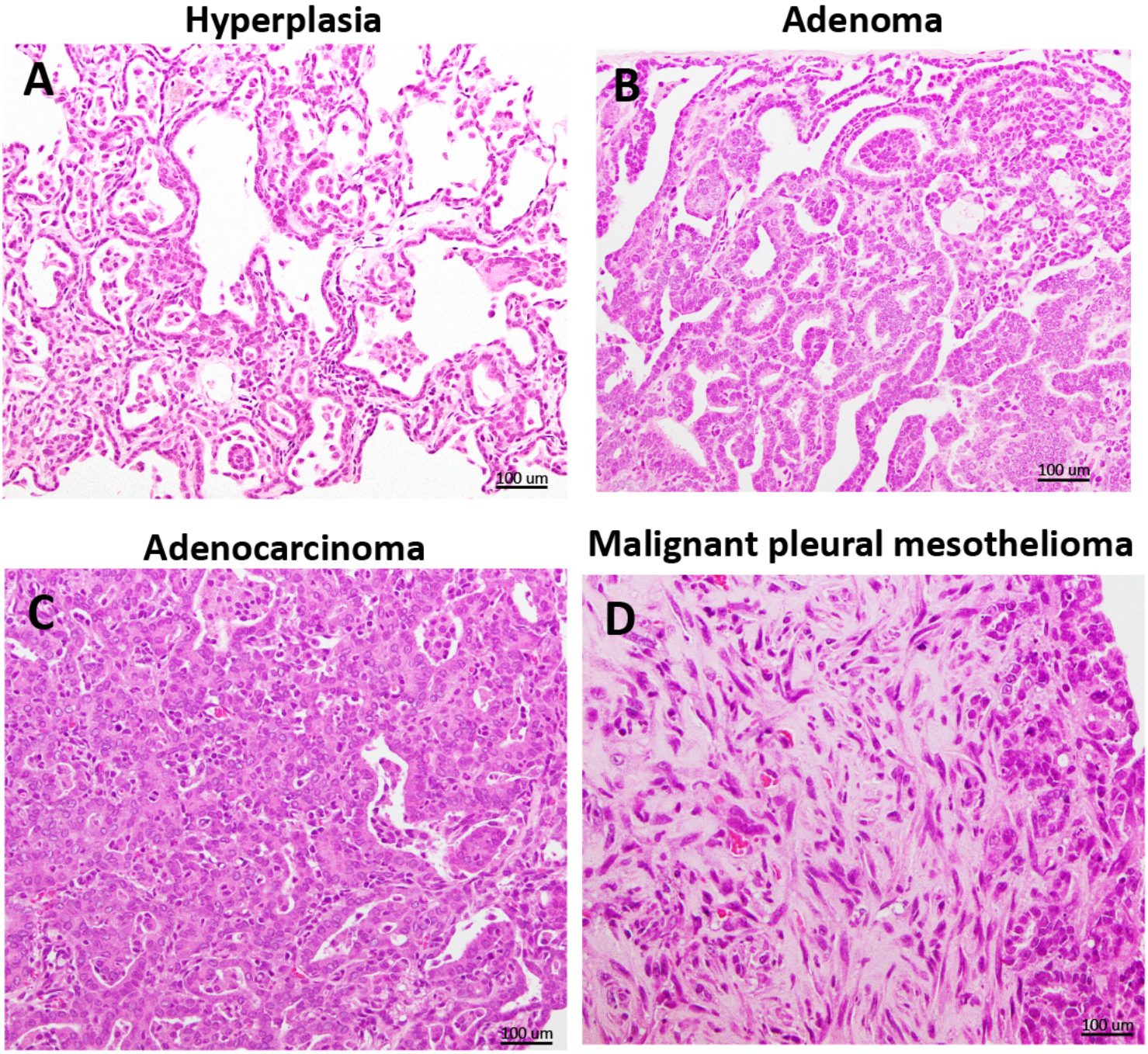

Figure 2

Representative preneoplastic and neoplastic lesions at 104 weeks. A Bronchiolo-alveolar hyperplasia, B Bronchiolo-alveolar adenoma, C Bronchiolo-alveolar adenocarcinoma, and D Malignant pleural mesothelioma.

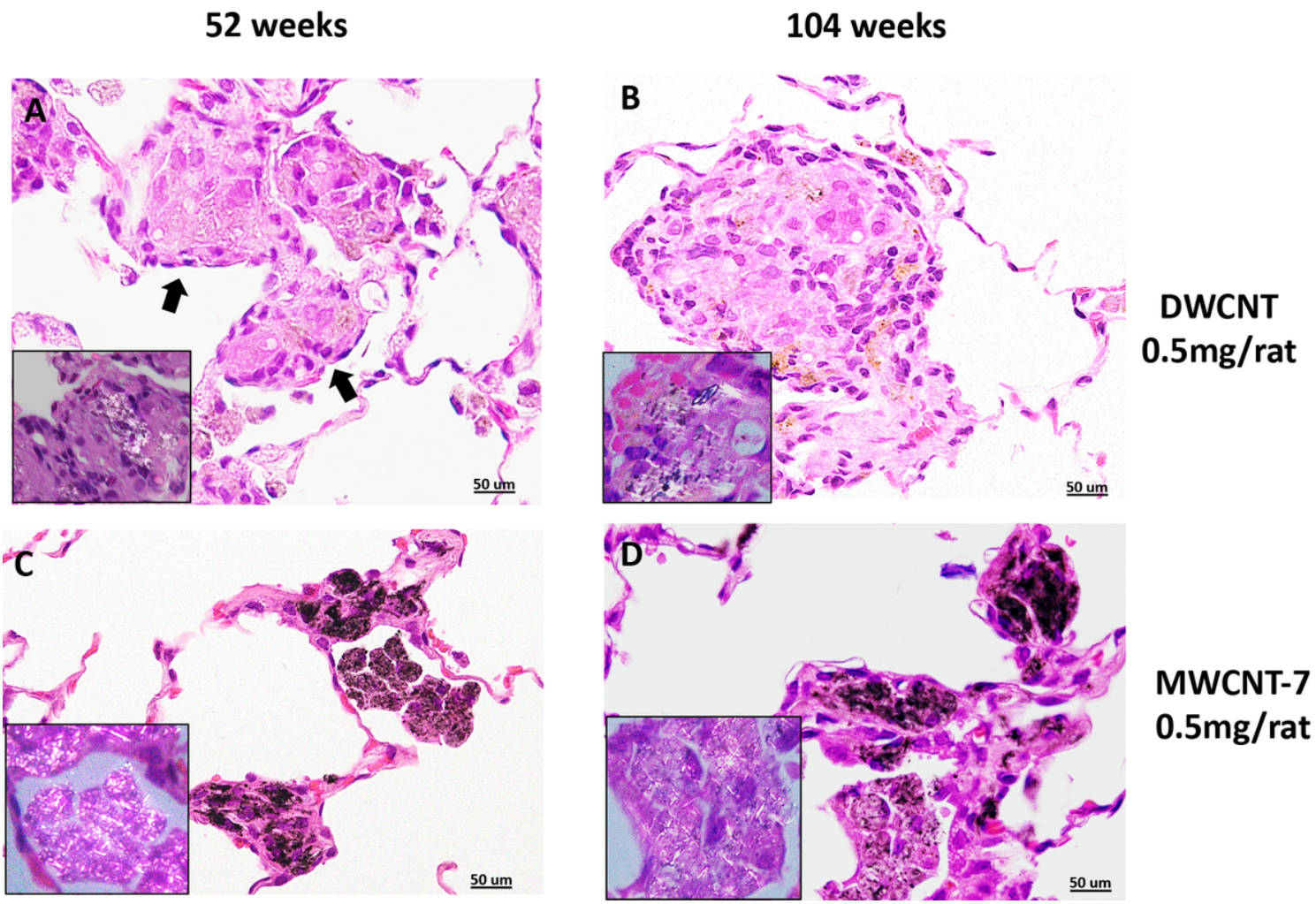

Figure 3

Lung sections of rats administered DWCNT (0.5 mg) at 52 weeks (A) and 104 weeks (B). The majority of the DWCNT is encapsulated in granulation tissue (arrows). The boxed areas are higher magnifications using a polarized lens showing DWCNT fibers. Lung sections of rats administered MWCNT (0.5 mg) at 52 weeks (C) and 104 weeks (D). MWCNT-7 can be seen encapsulated inside granulation tissue. In contrast to DWCNT, free macrophages phagocytosing MWCNT-7 fibers are a common feature. The boxed areas are higher magnifications using a polarized lens showing MWCNT fibers in free macrophages.

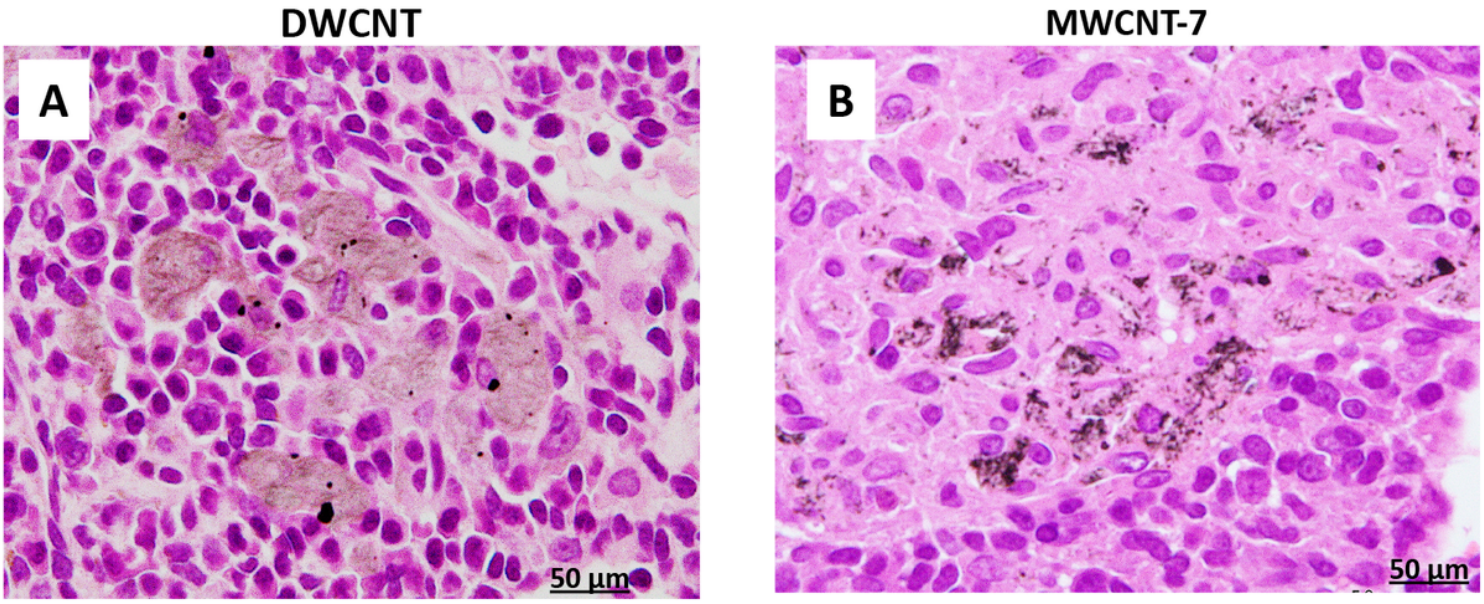

Figure 4

Mediastinal lymph nodes of rats administered 0.5 mg DWCNT (A) or 0.5 mg MWCNT-7 (B). Both fibers are shown to translocate from the alveoli to the mediastinal lymph nodes.

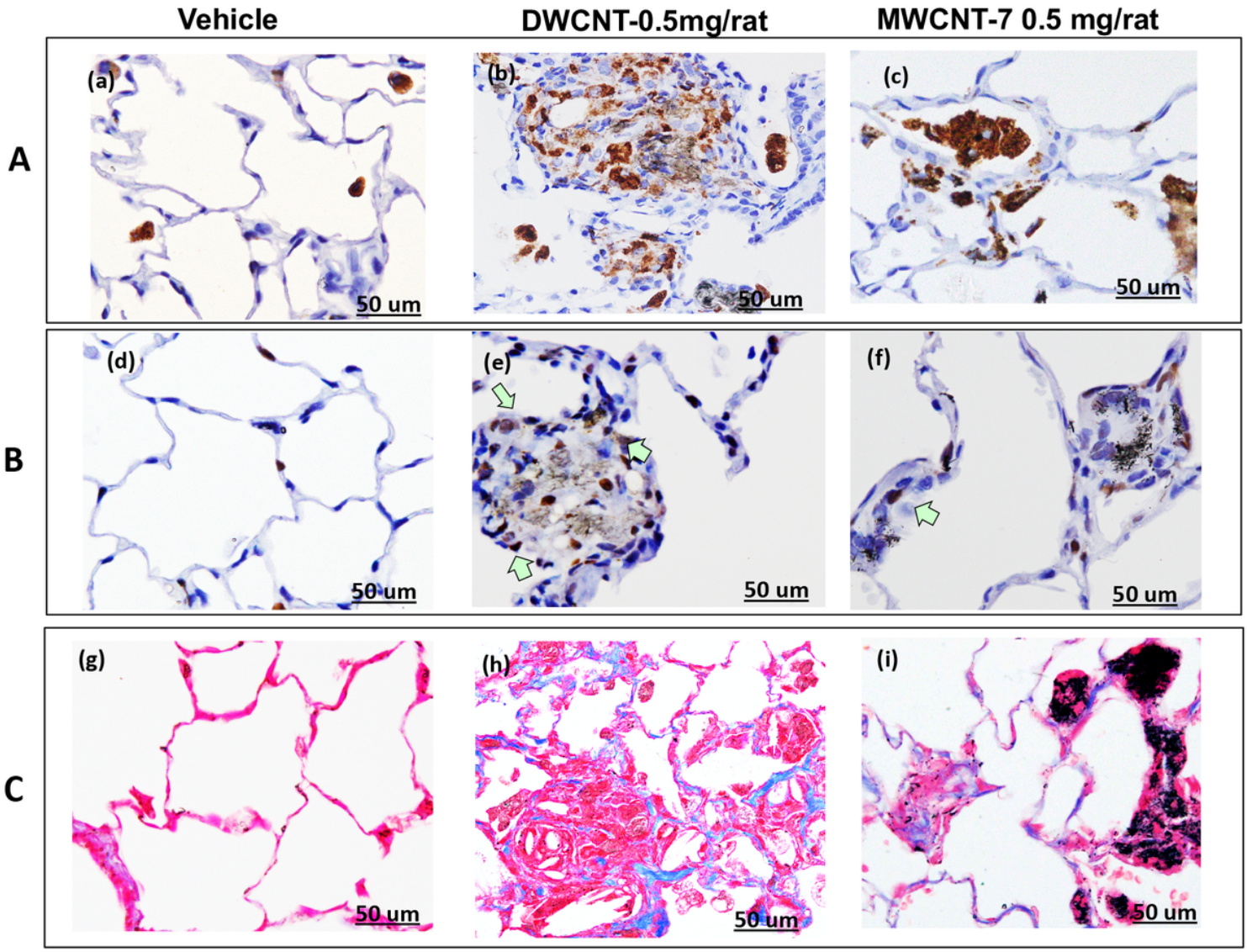

Figure 5

Panel A shows CD68 immunostaining of lung tissue from rats in the vehicle group (a), DWCNT 0.5mg group (b), and MWCNT-7 0.5 mg group (c) at 104 weeks. Panel B shows PCNA immunostaining of the lung tissue from rats in the vehicle group (d) , DWCNT 0.5mg group (e), and MWCNT-7 0.5 mg group (f) at 104 weeks. Panel C shows Masson's trichrome collagen staining of lung tissue from rats in the vehicle group (g) , DWCNT 0.5mg/rat group (h), and MWCNT-7 0.5 mg/rat group (i).

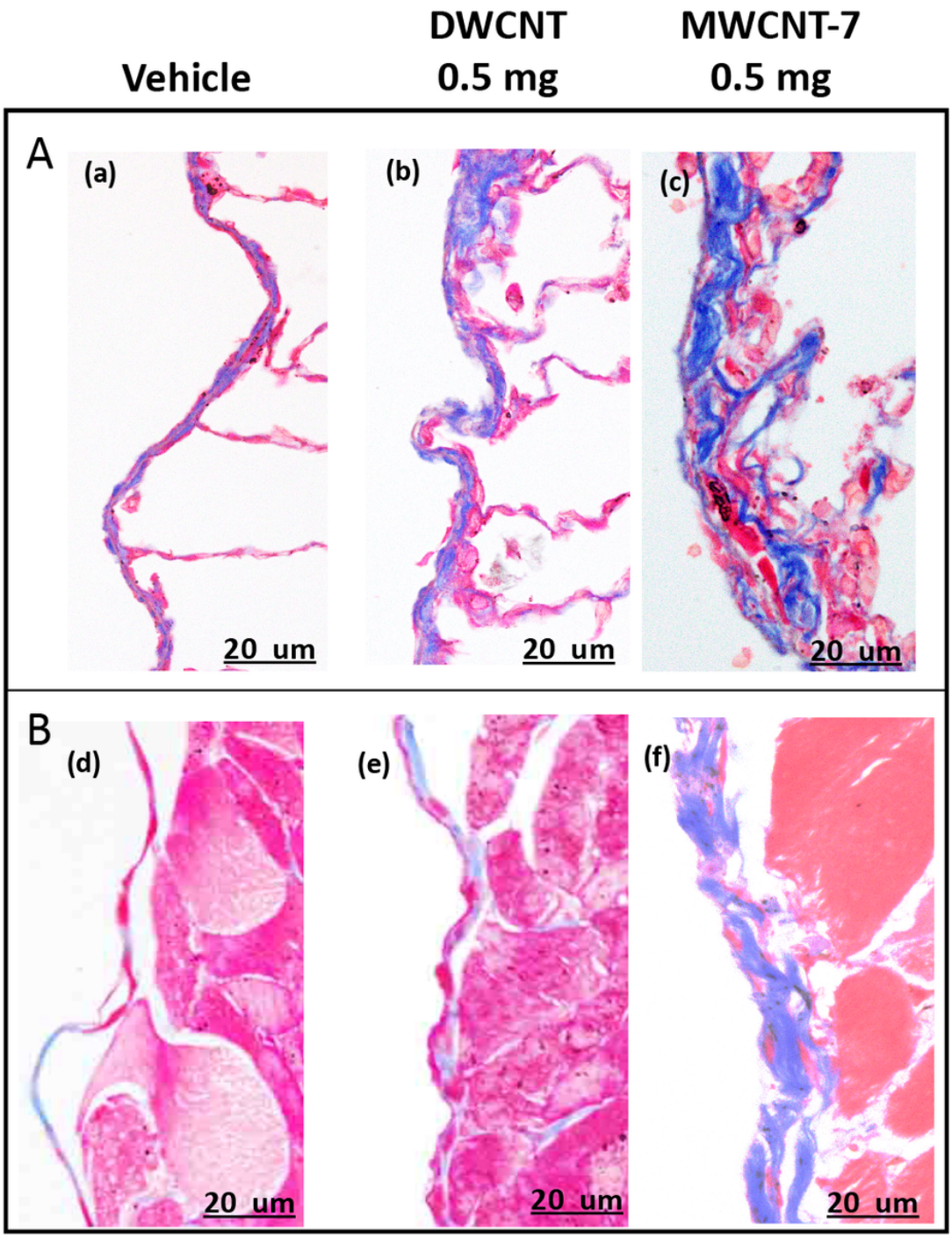

Figure 6

Panel A shows Masson's trichrome collagen staining of the visceral pleura of rats from the (a) Vehicle, (b) DWCNT 0.5mg, and (c) MWCNT-7 0.5 mg groups. Panel B shows Masson's trichrome collagen staining of the parietal pleura of rats from the (a) Vehicle, (b) DWCNT 0.5mg, and (c) MWCNT-7 0.5 mg groups.

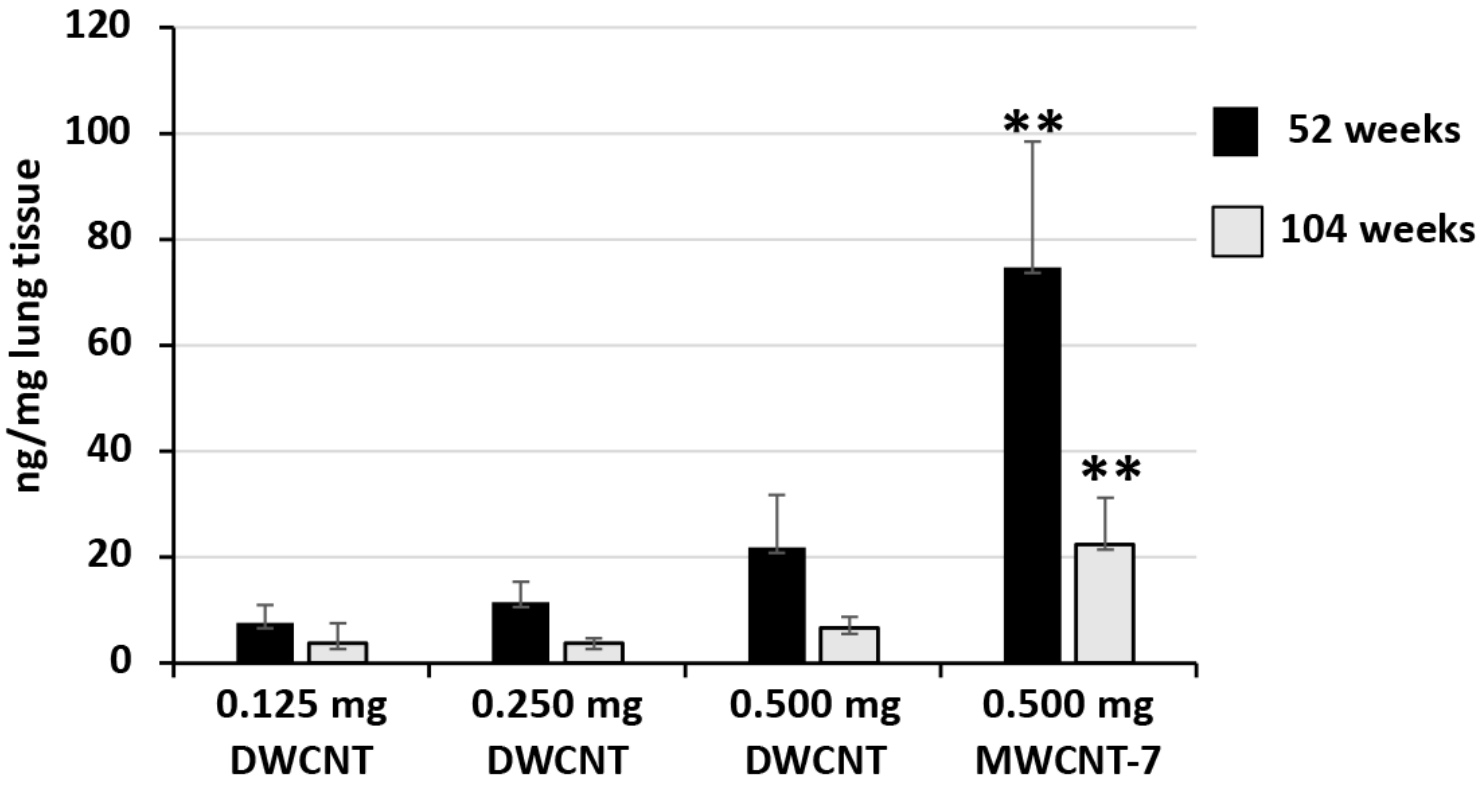

Figure 7

Lung tissue fiber burden at 52 and 104 weeks. ** p < 0.01 vs DWCNT (0.5mg)

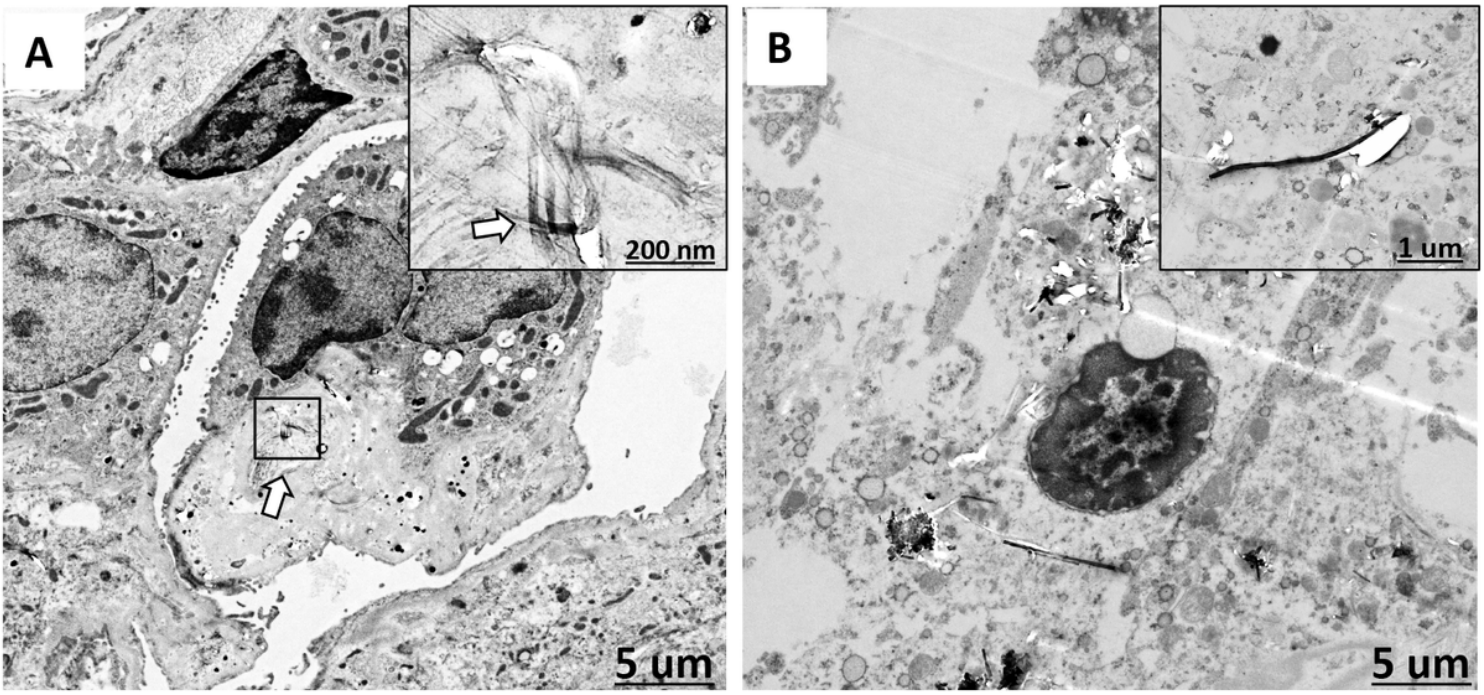

Figure 8

Panel A shows a TEM image of a rat lung treated with DWCNT (0.5mg) showing several very thin curved fibers (arrow and at higher magnification in the boxed area) engulfed by a macrophage with two nuclei. Panel B shows a

TEM image of rat lung treated with MWCNT-7 (0.5 mg) showing rigid fibers in the cytoplasm of an alveolar macrophage. Inset shows an enlarged view of an MWCNT-7 fiber in the macrophage cytoplasm.

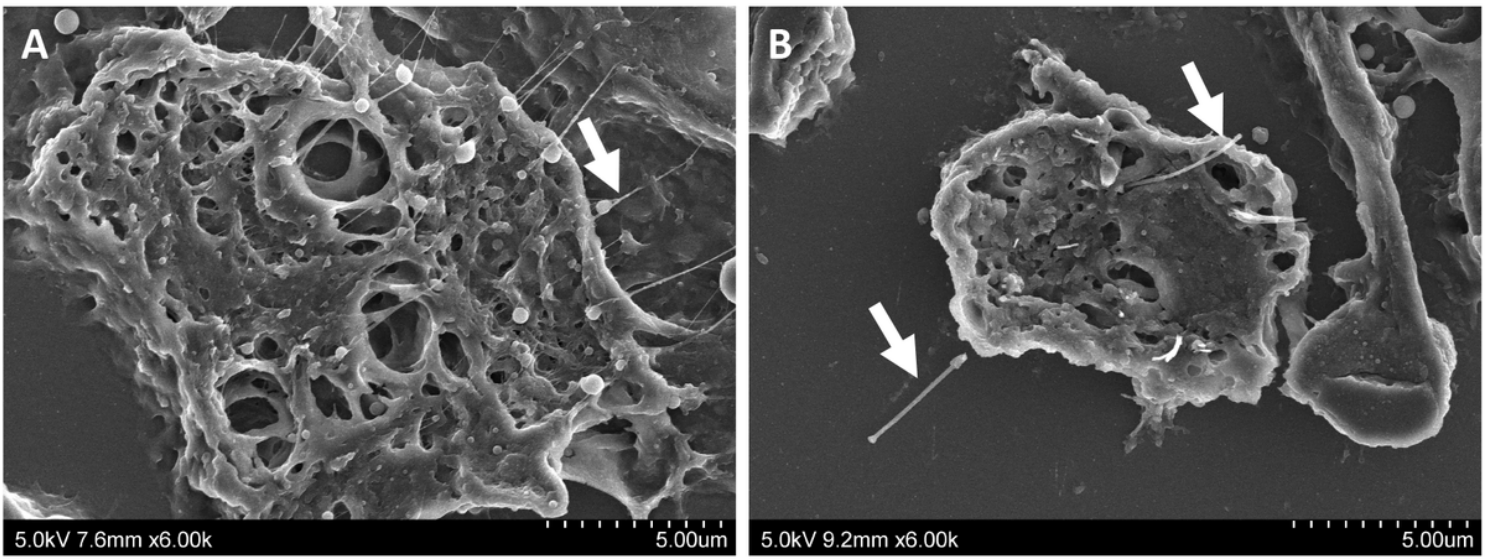

Figure 9

Panel A shows an SEM image of numerous thin DWCNT fibers (arrow) engulfed by a macrophage. Panel B shows an SEM image of a rigid MWCNT-7 fiber penetrating through the cell membrane of a macrophage (arrow). Free MWCNT-7 fibers were also observed in the alveolar space.

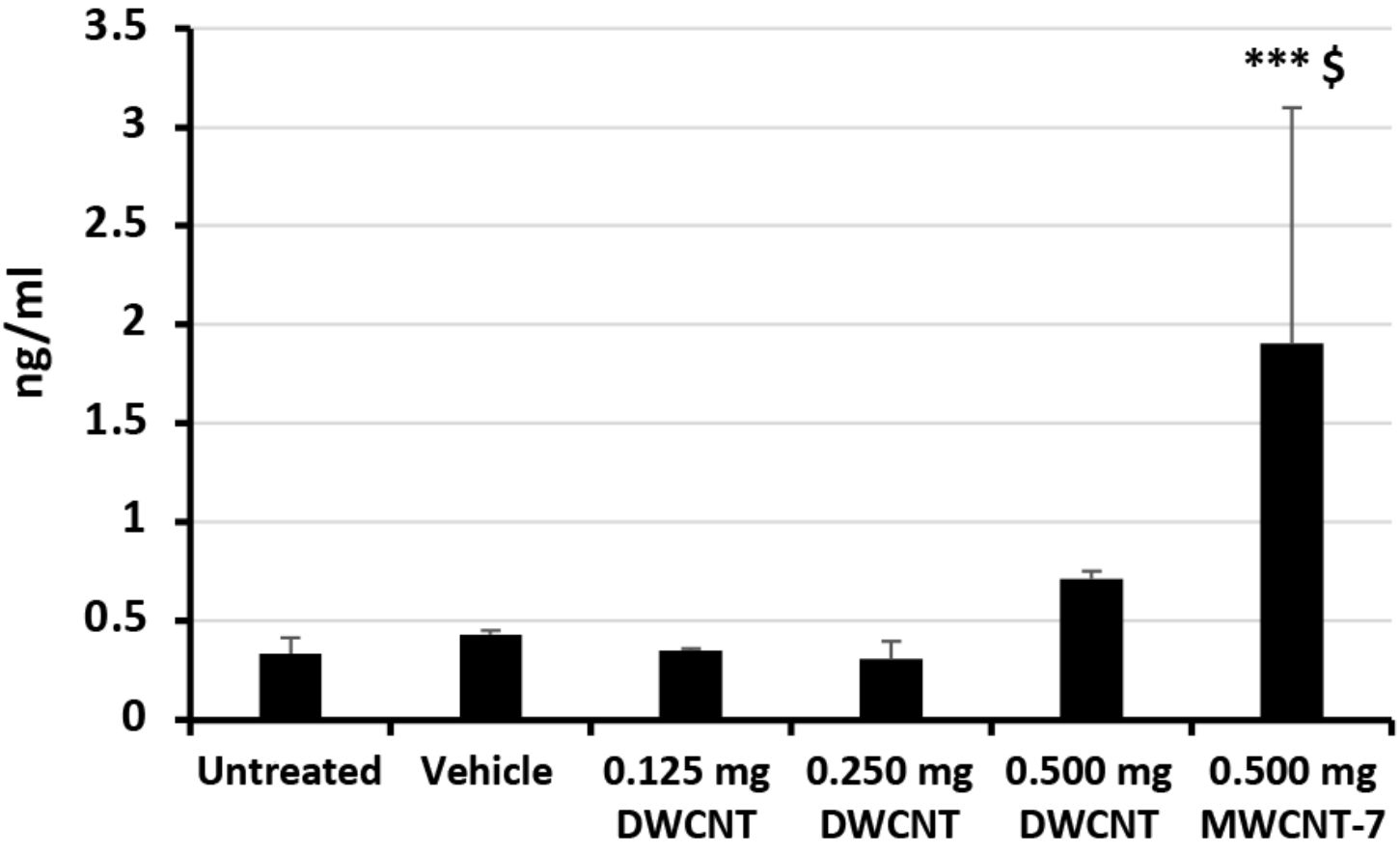

Figure 10

HMBG1 levels in the pleural lavage fluid at 104 weeks. *** p < 0.001 vs vehicle $p < 0.05 vs DWCNT (0.5mg)

Supplementary Files

This is a list of supplementary files associated with this preprint. Click to download.

- Additionalfile1.pdf
- Additionalfile2.pdf